

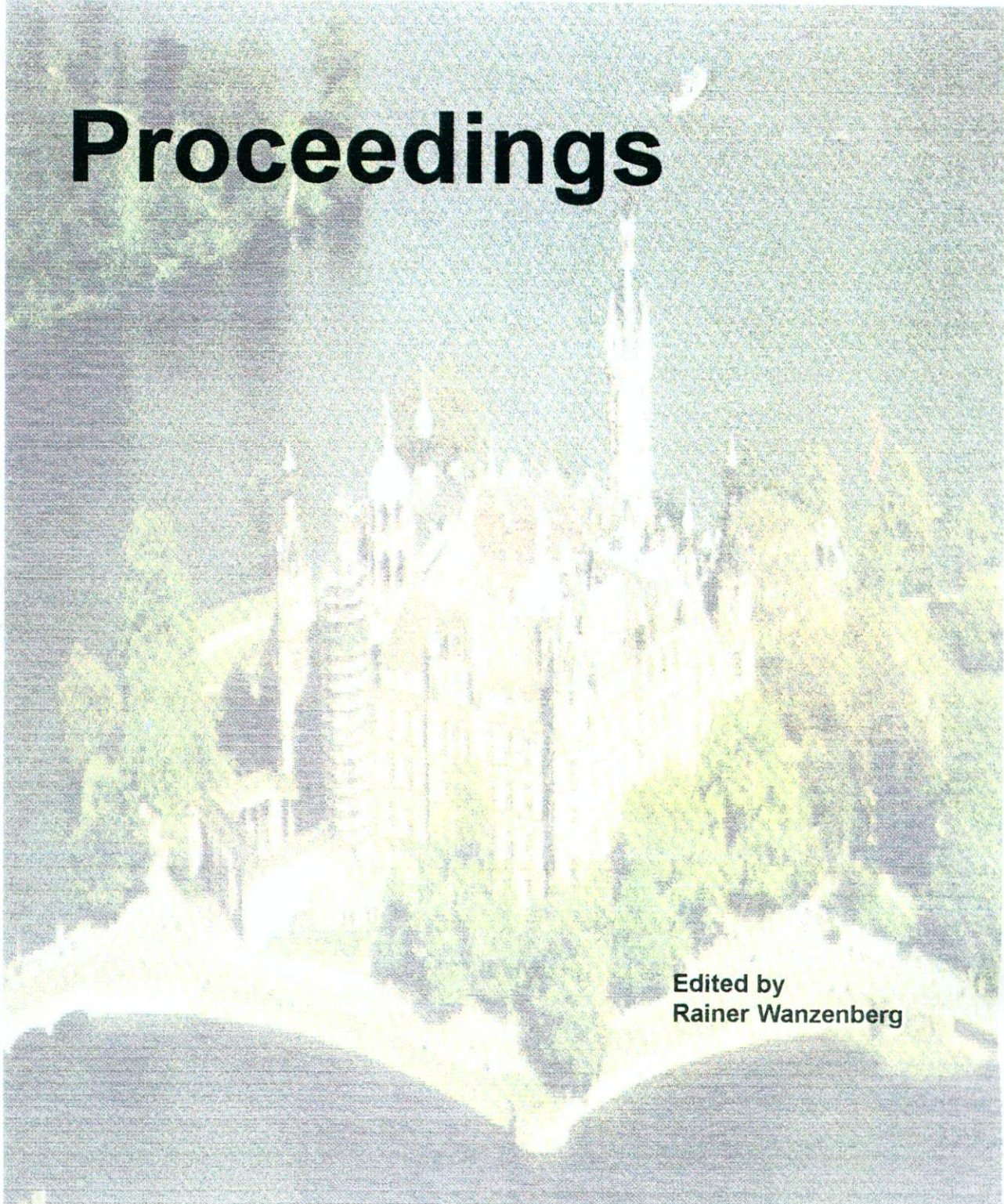
u B381.2  
S.75

# SOURCES '94

International Workshop  
on  $e^+e^-$  Sources and Pre-Accelerators for Linear Colliders

Schwerin, Germany, Sept. 29 - Oct. 4, 1994

## Proceedings



Edited by  
Rainer Wanzenberg

*Schwerin Palace, located downtown, about 3 km from the workshop hotel*

B381.2  
S. 75



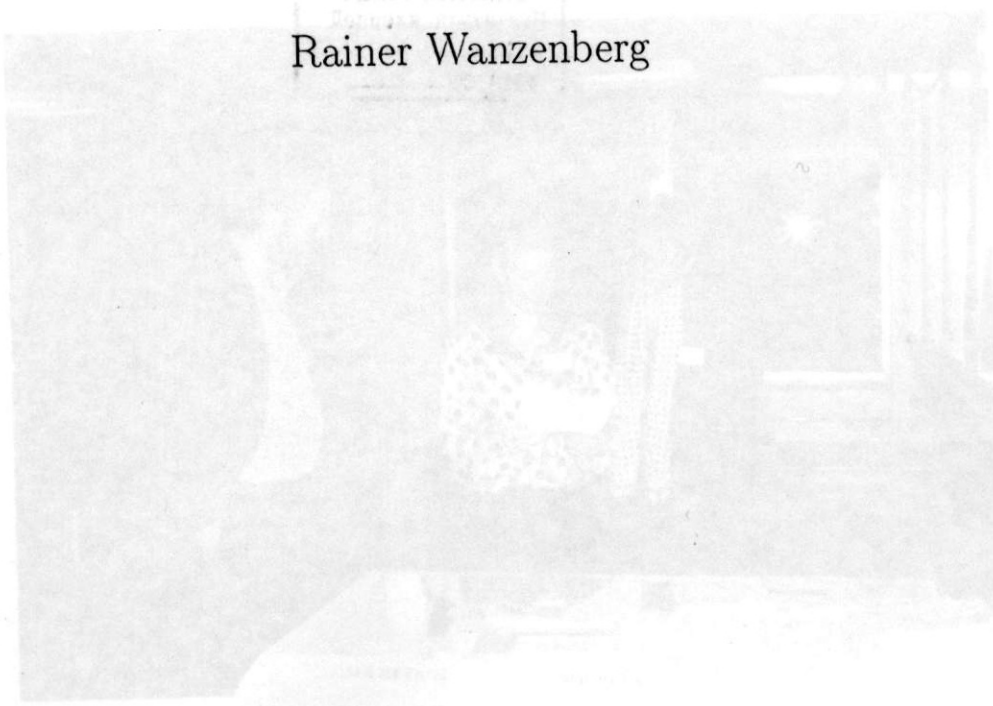
SOURCES '94

International Workshop  
on  $e^+ e^-$  Sources and Pre-Accelerators  
for Linear Colliders

Schwerin, Germany, Sept. 29 - Oct 4, 1994

Proceedings

Edited by  
Rainer Wanzenberg



# Polarized Positron Sources

Alexander Mikhailichenko  
Budker INP, Novosibirsk

September 30, 1994  
(Friday)

# Polarized Positron Sources<sup>1</sup>

A.A. Mikhailichenko  
Budker INP  
630090, Novosibirsk, Russia<sup>2</sup>

The collisions of both polarized electron and positron high energy beams is very attractive for fine physics beyond the standard model. Some schemes discussed what is able to prepare such a statement for future linear collider.

## 0. Introduction<sup>3</sup>

The importance of a polarization for high energy physics was discussed a lot of times by many authors. Even in simple treatment one can see the gain of factor 2 in output of an ordinary and routine reactions. This is due to the circumstance that high energy statement is a polarized one, so each particle of the beam looks only for an appropriate polarized one from incoming beam. Or with the other words, each particle can see only half of the particles from incoming beam. In [2] the importance of polarization for seeking new bosons beyond the Standard Model carefully discussed. The output made there is that at the energy range  $\sqrt{s} \approx 500 \text{ GeV}$  for the settings the  $Z'$  boson mass, the polarized beams gives the luminosity gain by  $\sim 5$  times, or with unpolarized beams the total energy need to be 2-3 times higher. This is impressive figure.

Requirements, arising from typical linear collider design, one can find, for example, in [3,4]. The general output of the requirements is that the power carried by the beams is of the order of few Megawatts. So the efficiency of the particle generation is one among important components of the any project. Some projects from the very beginning include the possibility to collide polarized particles, both electrons and positrons or the electrons only.

## 1. Polarized statements of electron and gamma radiation.

For description the electron polarization the usual convention is in defining the polarization vector  $\vec{P}$  (spin vector) in the rest frame of the positron or electron (see for example [5]). The fields are defined in the laboratory system. The equation of the spin motion can be represented as following [6]

$$\frac{d\vec{P}}{dt} = \frac{2\mu mc^2 + 2\mu'(E - mc^2)}{\hbar E} (\vec{P} \times \vec{H}) + \frac{2\mu'E}{\hbar(E + mc^2)} (\vec{E} \times \vec{P}) + \frac{2\mu mc^2 + 2\mu'E}{\hbar(E + mc^2)} (\vec{P} \times \vec{E})$$

where  $\vec{\beta} = \vec{v}/c$ ,  $c$  is a speed of light,  $\vec{E}$ ,  $\vec{H}$  are correspondly the electric and magnetic fields in the laboratory frame,  $E$  is the particle energy,  $t$  is the time in lab frame,  $\mu = -\frac{e\hbar}{2mc} = -9.3 \cdot 10^{-21} \text{ erg} \cdot \text{Gauss}$ ,  $\mu' \equiv \mu \frac{\alpha}{2\pi} = -1.1 \cdot 10^{-23} \text{ erg} \cdot \text{Gauss}$ ,  $\alpha = e^2 / \hbar c = 1/137$  is the fine structure constant,  $\hbar$  is the Plank constant.

<sup>1</sup> The paper presented on International Workshop on  $e^+, e^-$  Sources and Pre-Accelerators for LC. SOURCES 94, Schwerin, Germany, September 29 - October 4, 1994

<sup>2</sup> Temporary address: CERN, CH-1211, Geneva 23, Switzerland

<sup>3</sup> We shall see, that the methods of polarized positron generation, discussed below, can be applied to polarized electron generation with the same success. The question here only in the cost of the method applied, compared with the other one, used an appropriate photocathod, illuminated with polarized laser light [1].

Polarization of the photon defined by the matrix of polarization, where the components are the products of different components of the electrical field vector  $E_i E_j$ ,  $i, j = 1, 2$ .

Spin handling and management for the linear collider complex was considered in [7]. The manipulation with the spin is based on the anomalous magnetic moment  $\mu'$ , what yields the rotation the vector of spin with respect to the vector of momenta. The angular frequency, same as the frequency of the vector momenta particle has at the energy 440.6 MeV.

Depolarization in the interaction region was a subject of considerations from the very beginning [8 a,b]. Due to huge magnetic field of incoming beam the vector of spin rotates at the angle  $\varphi \approx 2\pi \cdot E[\text{GeV}] / 0.4406$  with respect to the vector of momenta. The very first estimations as well as the last one [9] shows that this effect yield a lost of a few percent of polarization and need to be taken into account.

## 2. Conversion of polarized gammas obtained from the wiggler.

Basically the idea [10] of polarized particles generation is rather simple. It is based on very well described components. The content of this idea is to irradiate the thin target with circularly polarized photons of sufficient energy and to collect the positrons at the top of its energy, Fig.1. Due to specific properties of interaction of the photons with the matter, the positrons at the high (or lower) energy top spectra has a longitudinal polarization. The source of radiation could be a primary one (helical wiggler or undulator) or the secondary one (back scattered photons). The target also could be treated as real material or the photon one. If the source is not polarized, then the output positrons or electrons are also not polarized.

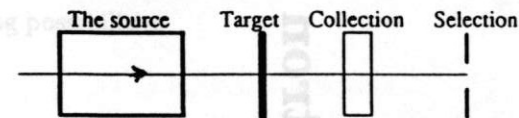


Fig. 1. The basis of conversion system for polarized particle production.

2.a. This idea with real helical wiggler was under consideration in [11-14]. In [15] one can find the latest results on this subject. On Fig. 2 there is represented more detailed view of the scheme with a wiggler.

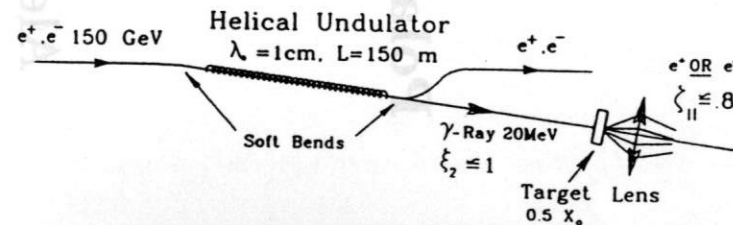


Fig. 2. The helical wiggler based scheme.

Let us make more detailed description of the elements of this scheme.

Interaction of the photons with the nuclei was described in many tutorials. We will use here [16,a,b] as a reference. The differential cross-section of the pair production by the photon has a rather complex dependence near the maximal possible positron (or electron) energy. Some additional difficulties connected with the screening the Coulomb field of the nuclei by the electrons. The screening becomes important when the minimal wavelength, connected with the momentum  $q_{min}$ , transferred to the nuclei, becomes bigger, than the size of the nuclei, i.e.  $\hbar/q_{min} \geq a_0 Z^{-1} \equiv \hbar^2 / e^2 m \cdot 1 / Z^{1/3}$ , where  $Z$  is the atomic number of the conversion target and it was substituted the Bohr radius value  $a_0 = \hbar^2 / e^2 m$ . This gives  $q_{min} \leq m c \alpha Z^{1/3}$ . Since

$q_{min} = p_+ + p_- - \hbar \omega / c = m c \frac{m c^2 \hbar \omega}{2 E_+ E_-}$ , where  $E_+$  is the positron total energy,  $E_- = E_+ - E$ , is the electron total energy,  $E_+ = \hbar \omega$  is the energy of the incoming photon, that yields  $\frac{m c^2 \hbar \omega}{2 E_+ E_-} \leq \alpha Z^{1/3}$ , or

$\chi = \frac{m c^2 \hbar \omega}{2 \alpha Z^{1/3} E_+ E_-} \leq 1$ . The parameter  $\chi$  describing the screening. Thus as we are interesting the situation, when  $E_+ = E_- = 20 MeV$ ,  $Z = 80$ ,  $\alpha Z^{1/3} \approx 0.03$ , so  $\chi = 32 m c^2 / E \gg 1$ , i.e. no screening. We will represent here an analytical expression what is valid in Born approximation [16a]

$$\frac{d\sigma(E_+, E_-)}{d(E_+ / E_+)} = 4 \alpha Z^2 r_0^2 G(E_+, E_-) = \alpha Z^2 r_0^2 \frac{p_+ p_-}{E_+^2} \left\{ -\frac{4}{3} - 2 E_+ E_- \frac{p_+^2 + p_-^2}{p_+^2 p_-^2} + m^2 c^4 \left( \frac{E_+ l_+}{p_+^3} + \frac{E_- l_-}{p_-^3} - \frac{l_+ l_-}{p_+ p_-} \right) + L \left[ \frac{E_+^2 (E_+^2 E_-^2 + p_+^2 p_-^2)}{p_+^3 p_-^3} - \frac{8 E_+ E_-}{3 p_+ p_-} - \frac{m^2 c^4 E_+}{2 p_+ p_-} \left( \frac{E_+ E_- - p_+^2}{p_+^3} l_- + \frac{E_+ E_- - p_-^2}{p_-^3} l_+ + \frac{2 E_+ E_- E_-}{p_+^2 p_-^2} \right) \right] \right\}$$

where  $\alpha = e^2 / \hbar c = 1/137$  is a fine structure constant,  $r_0 = e^2 / m c^2$  is the electron classical radius,  $l_{\pm} = \ln \frac{E_{\pm} + p_{\pm}}{m c^2}$ ,  $L = \ln \frac{E_+ E_- + p_+ p_- + m^2 c^4}{m c^2 E_+}$  and the relation between the energy and momentum is the following  $p_{\pm}^2 = E_{\pm}^2 - m^2 c^4$  ( $c$  included in  $p$ , definition of [16a]). This cross-section dependence has a view, represented on the Fig. 3A. It is clear, that the spectral density goes to zero, when  $E_+$ , or  $E_-$  goes to the maximum possible (or the lowest) value. When the  $E_+, E_-, E_+ \gg 2 m c^2$  the angles of electron and positron with respect to direction of the photon incident have the order  $\theta_{\pm} = m c^2 / E_{\pm}$  and formula looks like

$$\frac{d\sigma(E_+, E_-)}{d(E_+ / E_+)} \approx 4 \alpha Z^2 r_0^2 \ln(183 / Z^{1/3}) \hat{G}(E_+ / E_+) \approx \frac{A}{N_0 X_0} \hat{G}(E_+ / E_+),$$

where  $A$  is its atomic weight,  $N_0 \approx 6.022 \cdot 10^{23}$  is the Avogadro number, radiation length  $X_0$  is defined by

$$X_0^{-1} \approx 4 r_0^2 \alpha \frac{N_0}{A} Z^2 \ln \left( \frac{183}{Z^{1/3}} \right) [cm^2 / gramm],$$

function  $G(x)$  has a rather simple form in this case

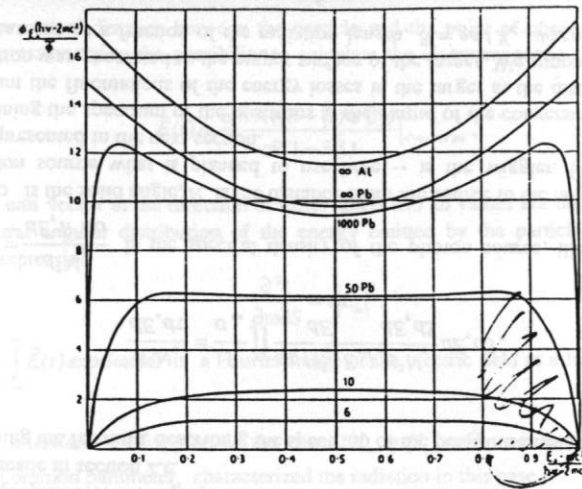


Fig. 3A. The differential cross-section of the pair production  $\frac{E_+ - 2 m c^2}{\alpha Z^2 r_0^2} \frac{d\sigma(E_+, E_-)}{dE}$  as the function of the positron partition energy  $y = \frac{E_+ - m c^2}{E_+}$  [16a]. The numbers at the top of each curve indicates the energy of incoming quanta in units  $m c^2$ . The curves for  $E_+ = 6, 10 m c^2$  are valid for any element.

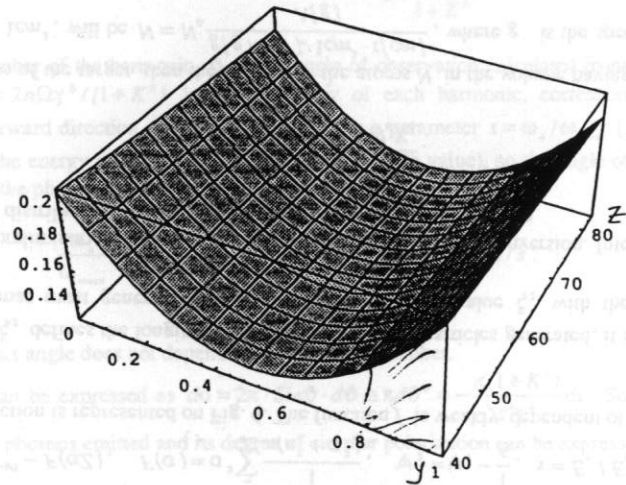


Fig. 3B. The differential cross-section of the pair production  $\frac{E_+}{4 \alpha Z^2 r_0^2} \frac{d\sigma(E_+, E_-)}{dE}$  as the function of the positron partition energy  $y = \frac{E_+}{E_+}$  when  $E_+, E_-, E_+ \gg 2 m c^2$

163-

$$\hat{G}(x) = x^2 + (1-x)^2 + \frac{2}{3}x(1-x) - \frac{x(1-x)}{9 \ln(183Z^{-1/3})}$$

This function is represented on Fig. 3B. There is no dependence of the incoming photon energy in this function, the ratio only. This is sequence of the assumption  $E_+, E_-, E_+ \gg 2mc^2$  or when the energy of each particle far from the limit arising from the energy conservation law.

The values at the boundary condition, when  $E_+, E_- = E_\gamma$ , the function  $G \rightarrow 0$ . For analytical calculations, in more realistic case of intermediate energies of gammas this function can be approximated as having a root dependence. For example, for  $E_\gamma = 50mc^2$ ,  $Z = 82$  this function can be represented [12] as

$$G(x) = \begin{cases} 4.75\sqrt{x}, & 0 \leq x < 0.11 \\ 1.55, & 0.11 < x < 0.89 \\ 4.75\sqrt{1-x}, & 0.89 < x \leq 1 \end{cases}$$

One can see, that the number of the particles here is lower than for intermediate partial energies. As the method requires to collect the particles near the top of the energy, this circumstance reduces the efficiency of positron generation. In any case the higher energy is desirable from the point of conversion efficiency. For example, the increasing the energy of incoming photos from 5 to 25 MeV yields increasing the efficiency about 6 times.

The mostly important property of the pair generation by the polarized photon, is the transferring the polarization from the gamma to the positron and electron created. Basically this is a sequence of the conservation law for the momentum. The polarization phenomena in positron production is carefully investigated in [17]. The longitudinal polarization of the particle created is a function of its energy,  $E_+, E_-$  and the polarization  $\xi_2$  of the incoming gamma

$$\bar{\xi} = \xi_2 \cdot [f(E_+, E_-) \cdot \bar{n}_1 + g(E_+, E_-) \cdot \bar{n}_2] = \bar{\xi}_1 + \bar{\xi}_2$$

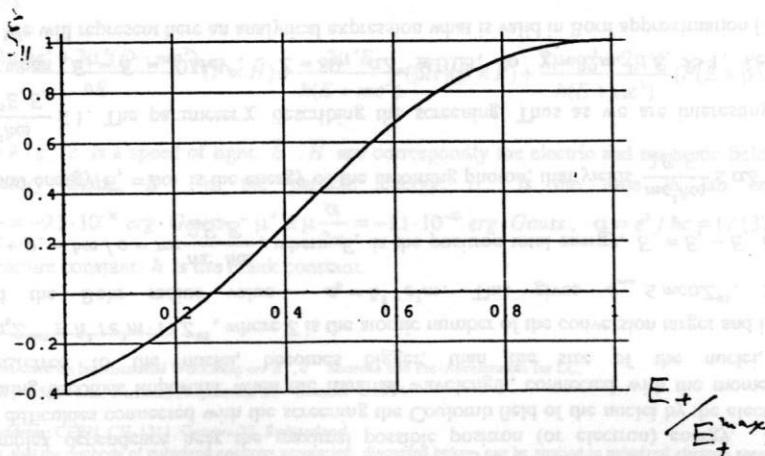


Fig. 4. The longitudinal polarization of the positron created as a function of its fractional energy [17].

where  $\bar{n}_1$  is directed along the initial direction of the gamma radiation and  $\bar{n}_2$  is rectangular to it. An analytical expression for  $f$  has a form

$$f = E_+ \frac{E_+ \psi_1 - E_- (\psi_1 - 2\psi_2/3)}{(E_+^2 + E_-^2) \psi_1 + 2E_+ E_- / 3} = \frac{x \psi_1 - (1-x)(\psi_1 - 2\psi_2/3)}{(x^2 + (1-x)^2) \psi_1 + 2x(1-x)/3}$$

where  $\psi_1 = \ln 183Z^{-1/3} - F(\alpha Z)$ ,  $F(\sigma) = \sigma^2 \sum_{n=1}^{\infty} \frac{1}{n(n^2 + \sigma^2)}$ ,  $\psi_2 = \psi_1 - \frac{1}{6}$ ,  $x = E_+ / E_\gamma$ .

The view of this function is represented on Fig. 4. The function  $f$  is weakly dependent of  $Z$ .

As the polarization  $\xi_2$  defines the longitudinal polarization of the particles generated, it is clear that the source of gammas must generate them with highest possible value  $\xi_2$  with the necessary amount.

Let us make preliminary estimation of the efficiency of the gamma conversion. Integrating the formula for spectral distribution, one can obtain the cross-section per one atom

$$\sigma_\omega \equiv \int_0^1 \frac{A}{N_0 X_0} G(x) dx \equiv \frac{7}{9} \frac{A}{N_0 X_0}$$

If  $t$  is the thickness of the target, then the number of the atoms  $N$  in the volume having a height  $t$  and a cross-section  $1 \text{ cm}^2$ , will be  $N = N_0 \frac{g [g / \text{cm}^3] \cdot 1 \text{ cm}^2 \cdot t [\text{cm}]}{A [g]}$ , where  $g$  is the specific weight

of the target material. So the number of the positrons what will be created at the exit of the target will be  $N_+ \equiv N_+ \sigma_\omega N \equiv \frac{7}{9} N_+ \frac{g t}{X_0} = \frac{7}{9} N_+ \tau$ , where  $\tau = \frac{g t}{X_0}$  is the target length, measured as a fraction

of the radiation length. We will be interesting in  $\tau \leq 0.5$  and taking into account that about 1/5 positrons only carrying the necessary level of polarization, we can finally estimate the conversion efficiency of the photons as  $N_+ / N_\gamma = 0.077$ , or 7.7%. This estimation looks very close to that obtained from numerical calculation (see lower). We supposed also, that the phase volume of the positrons created, corresponds mostly to multiscattering in a target, and the particles could be accepted by appropriate collecting system. The conditions for acceptance is a subject of special considerations made in section 2.c.

For obtaining the formula, describing the spectrum of the positrons created, we can write

$$\frac{d^2 N_+}{dE_+ d\tau} = \frac{1}{\sigma_\omega} \iint \frac{d\sigma(E_+, E_-)}{dE_+} \frac{d^2 N_\gamma}{dE_\gamma dS} dE_\gamma dS$$

where  $\frac{d^2 N_\gamma}{dE_\gamma dS} = \frac{d^2 N_\gamma}{dE_\gamma R^2 d\Omega}$  is the spectral density of the photon source, illuminating the target,

$dS = R^2 d\Omega$ ,  $d\Omega$  is the solid angle,  $R$  is the distance from the source to the target.

The photon source what is planned to use here -- is the wiggler. Formulas for wiggler radiation are represented in the next section.

For obtaining the spectrum of the positrons at the output of the conversion target, we need to take into account the fluctuations of the energy losses in the target at the distance from the point, where the positron was generated to the output surface of the target. We suppose that the target has a thickness, measured as a fraction of the radiation length,  $\delta = g d / X_0$ , where  $d$  is a geometrical

thickness (measured from the front surface of the target). The probability  $WdE_+$ , that the positron, created by the photon at the depth  $\tau$  with initial energy  $E_+$ , will have the energy in the interval from  $E_+^m$  to  $E_+^m + dE_+^m$  at the output of the target, is described by the formula [48]

$$W(E_+, E_+^m, \delta - \tau) dE_+^m = \frac{dE_+^m}{E_+} \cdot \left( \ln \frac{E_+}{E_+^m} \right)^{(\delta - \tau) - 1} / \Gamma(\delta - \tau),$$

where  $\Gamma(x) = \int_0^\infty t^{x-1} e^{-t} dt$  is the Gamma function. So, the number of the positrons, generated by the photon flux, having spectral-angular density  $d^2N_+ / dE_+ dS$ , and with the initial energy in the interval from  $E_+$  to  $E_+ + dE_+$  and leaving the converter at the energy interval from  $E_+^m$  to  $E_+^m + dE_+^m$  is [11,12]

$$\frac{d^2N_+}{dE_+ dE_+^m} = \int \frac{d^2N_+}{dE_+ dS} \cdot \exp(-\frac{7}{9}\tau) \cdot W(E_+, E_+^m, \delta - \tau) d\tau,$$

where the factor  $\exp(-\frac{7}{9}\tau)$  reflects the photon flux attenuation by the target.

Finally, the energy spectrum at the output of the target becomes

$$\frac{d^2N_+}{dE_+^m} = \int \frac{d^2N_+}{dE_+ dE_+^m} dE_+ = \frac{1}{\sigma_m} \int \frac{d\sigma(E_+, E_+)}{dE_+} \frac{d^2N_+}{dE_+ dS} \cdot \exp(-\frac{7}{9}\tau) W(E_+, E_+^m, \delta - \tau) d\tau dE_+ dE_+^m dS$$

Temporary we leave this formula until the end of the next section, where the detailed properties of the photon source are investigated.

The main requirements for the photon beam is the monochromaticity and sufficient flux, because even simple estimations made, indicates the necessity for about 15 initial photons for the one positron to be generated. We will see that the undulator radiation satisfy this requirement.

**Types of the undulators.** In general case, the wiggler generates the axis field type as the following

$$\vec{H}_1(z) = \vec{e}_x H_m \cos \frac{2\pi z}{\lambda_u} + \vec{e}_y H_m \sin \frac{2\pi z}{\lambda_u},$$

where  $x, y$  are the transverse coordinates,  $z$  is the longitudinal one,  $\lambda_u$  is the period of the wiggler,  $H_m, H_m$  are the magnetic field amplitudes in corresponding directions. The transverse motion is characterized [19] by relative velocities

$$\vec{\beta}(t') = (\beta_m \cos \Omega t', -\beta_m \sin \Omega t', \bar{\beta} - (\delta\beta)_m \cos 2\Omega t')$$

and the radius vector

$$\vec{r}(t') = \{x_m \sin \Omega t', y_m \cos \Omega t', \bar{\beta} c t' - (\delta z_m) \sin 2\Omega t'\},$$

where

$$\Omega = 2\pi \bar{\beta} c / \lambda_u, \quad \beta_m = H_m / H_c, \quad \beta_m = H_m / H_c, \quad (\delta\beta)_m = (\beta_m^2 - \beta_m^2) / 4, \quad x_m = c\beta_m / \Omega, \\ y_m = c\beta_m / \Omega, \quad \delta z_m = c(\delta\beta)_m / 2\Omega, \quad \bar{\beta} = \beta(1 - \beta_m^2 / 4), \quad \beta_m = (\beta_m^2 + \beta_m^2)^{1/2}, \\ H_c = 2\pi m c^2 / e \lambda_u \approx 10700 [G \cdot cm] / \lambda_u [cm], \quad t' = t - R(t') / c \text{ is the time in the moment of}$$

radiation,  $R$  is an actual distance between the particle and the point of observation,  $c$  is speed of light. These expressions give the possibility to calculate the electromagnetic field, radiated by the particle

$$\vec{E}(t) = \frac{e(\vec{n} \times ((\vec{n} - \vec{\beta}) \times \dot{\vec{\beta}}))}{cR(1 - \vec{n}\vec{\beta})} \Big|_{t' = t - R/c},$$

where  $\vec{n}$  is the unit vector in the direction of observation and all values are taken in the moment of radiation. Spectral angular distribution of the energy emitted by the particle on the area  $dS$  is determined by expression

$$\frac{\partial^2 \epsilon}{\partial \omega \partial S} = c |\vec{E}_\omega|^2,$$

where  $\vec{E}_\omega = \frac{1}{2\pi} \int \vec{E}(t) \exp(i\omega t) dt$  is a Fourier image of the electric field as a function of the time of observation  $t$ .

**Helical undulator or wiggler.** In the case  $H_m = H_m = H$ , we obtain circularly polarized radiation. The common parameter, characterized the radiation in this case is

$$K = \beta \gamma = e H \lambda_u / 2\pi m c^2 \approx 93.4 \cdot H [Tesla] \lambda_u [m].$$

This is so called deflection parameter or the undulatority factor.

For ultrarelativistic particle the frequency of radiation  $\omega$  is a function of the angle of observation and the  $K$  value

$$\omega_n = \frac{n\Omega}{1 - \vec{\beta}\vec{n}} \approx \frac{2n\Omega\gamma^2}{1 + K^2 + \gamma^2\vartheta^2} = \frac{\omega_{nmax}}{1 + \frac{\gamma^2\vartheta^2}{1 + K^2}},$$

where  $n$  is the number of the harmonic,  $\vartheta$  is the angle of observation calculated from the forward direction,  $\omega_{nmax} = 2n\Omega\gamma^2 / (1 + K^2)$  is the frequency of each harmonic, corresponding to the radiation in the forward direction, i.e.  $\vartheta = 0$ . We will use a parameter  $s = \omega_n / \omega_{nmax}$  [11,12] (what is the fraction of the energy with respect to its maximal possible value), so the angle of observation and the energy of the photon are connected by the relation

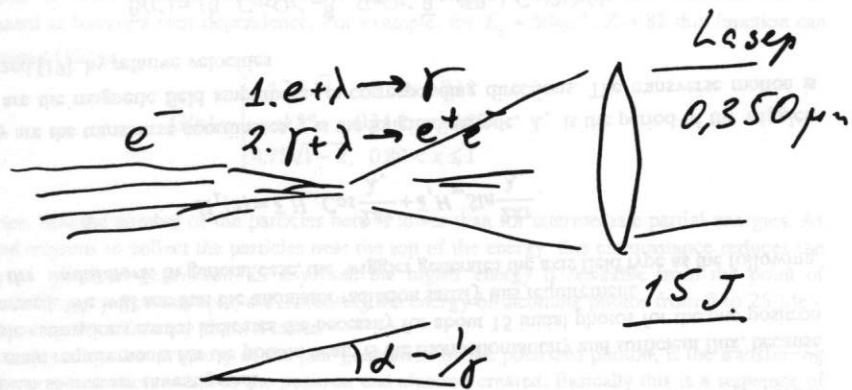
$$\frac{\omega_n}{\omega_{nmax}} = s = \frac{1}{1 + \frac{\gamma^2\vartheta^2}{1 + K^2}}, \text{ or } \gamma\vartheta = \sqrt{(1 + K^2)(1 - s)} / s.$$

Notice here that this angle does not depend of the harmonic number.

The solid angle can be expressed as  $d\Omega = 2\pi \cdot \sin\vartheta \cdot d\vartheta \approx \pi d\vartheta^2 = -\frac{\pi(1 + K^2)}{s^2\gamma^2} ds$ . So the spectral distribution of the photons emitted and its degree of circular polarization can be expressed as follows [11,12,19]

$$\frac{dN_n}{ds} = \frac{\pi(1 + K^2)}{s^2\gamma^2} \frac{dN_n}{d\Omega} = 4\pi\omega_n M \frac{K^2}{1 + K^2} F_n(K, s),$$

$$\xi_{2n} = \frac{\sqrt{1 + K^2}}{K} \frac{2s - 1}{\sqrt{s(1 - s)}} \frac{J_n(nK) J'_n(nK)}{F_n(K, s)},$$



where  $\kappa = 2K\sqrt{s(1-s)/(1+K^2)}$ ,  $F_n(K,s) = J_n'^2(n\kappa) + \frac{1+K^2(2s-1)^2}{4K^2 s(1-s)} J_n^2(n\kappa)$ ,  $J_n$  and  $J_n'$  is the Bessel function and its derivative,  $M$  is the number of the wiggler periods,  $\alpha = e^2/\hbar c = 1/137$  is a fine structure constant.

In dipole approximation,  $K \leq 1$ , using expansion of the Bessel function, we came to expressions [11]

$$F_n(K,s) = \frac{(nK)^{2n-1}}{2(n-1)!(n-1)!} \left( \frac{s(1-s)}{1+K^2} \right)^{n-1} \left( 1 - 2s + 2s^2 - \frac{2n}{n+1} \cdot \frac{K^2}{1+K^2} s(1-s)/1 + n(1-2s+2s^2) \right)$$

$$\xi_{2n}(K,s) = \frac{(2s-1) \left( 1 - \frac{2n^2+1}{n+1} \cdot \frac{K^2}{1+K^2} s(1-s) \right)}{\left( 1 - 2s + 2s^2 - \frac{2n}{n+1} \cdot \frac{K^2}{1+K^2} s(1-s)/1 + n(1-2s+2s^2) \right)}$$

On Fig. 5 there is represented the polarization as a function of  $K$ ,  $s$ .

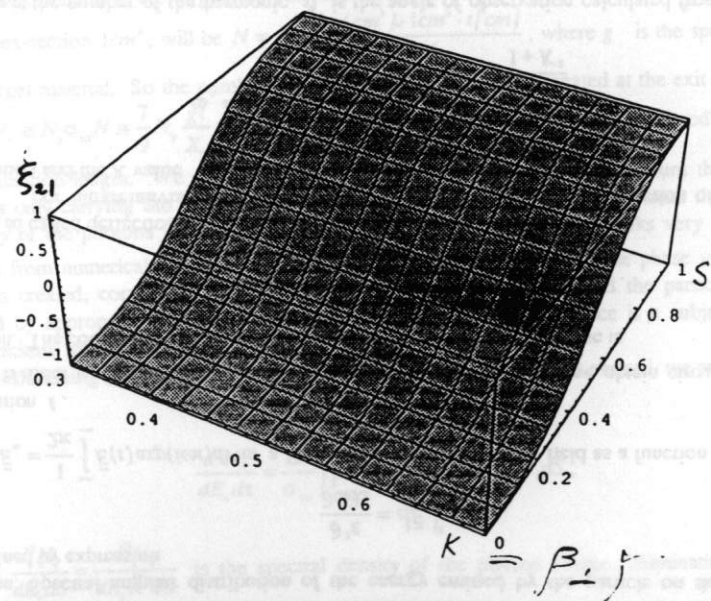


Fig. 5A. The polarization of the radiation emitted as a function of the  $K$  and  $s = \omega_e/\omega_{max}$  for the first harmonic.



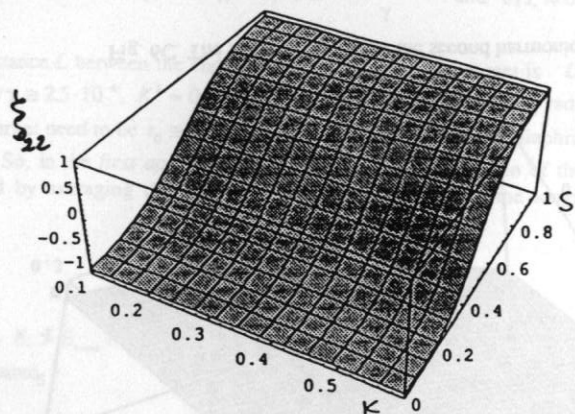


Fig. 5B. The polarization of the radiation emitted as a function of the  $K$  and  $s = \omega_+ / \omega_{max}$  for the second harmonic.

For harmonics  $n = 1, 2$  in approximation  $K^2 \ll 1$  it follows from here

$$F_1(K, s) \equiv \frac{1}{2}(1 - 2s + 2s^2), \quad F_2(K, s) \equiv 2s(1 - s)(1 - s + 2s^2)K^2, \quad \xi_{21} = \xi_{22} = \frac{2s - 1}{1 - 2s + 2s^2}.$$

These expressions as a function of the angle can be represented as

$$F_1(\vartheta) = \frac{1 + \gamma^2 \vartheta^2}{2(1 + \gamma^2 \vartheta^2)^2}, \quad F_2(\vartheta) = 2(K\gamma\vartheta)^2 \frac{1 + \gamma^4 \vartheta^4}{(1 + \gamma^2 \vartheta^2)^4}, \quad \xi_{21} = \xi_{22} = \frac{1 - \gamma^4 \vartheta^4}{1 + \gamma^4 \vartheta^4}.$$

One can see from expression for angular dependence of polarization, that the polarization becomes linear ( $\xi_{21} = \xi_{22} \equiv 0$ ), when the angle of observation  $\vartheta \equiv 1/\gamma$ .

Let us compare this angle with the maximal angular spread of the particles in the beam. The last is given by expression  $\vartheta_m \equiv \sqrt{\gamma\epsilon} / \gamma\beta_+$ , where  $\gamma\epsilon$  is a normalized emittance,  $\beta_+$  is an envelope function value in the wiggler. As the envelope function is of the order of the wiggler length  $\beta_+ = 100 \text{ m}$ , then for  $\gamma\epsilon = 10^{-4} \text{ cm} \cdot \text{rad}$ ,  $\gamma = 4 \cdot 10^5$  (200 GeV),  $1/\gamma \approx 2.5 \cdot 10^{-6}$ , one can estimate  $\vartheta_m \equiv \sqrt{10^{-4} / 4 \cdot 10^5} \approx 1.6 \cdot 10^{-7}$ , so  $\gamma\vartheta_m \approx 0.06$ . Thus there is no input to the photon flux on the target due to the angular spread in the beam. The beam dimensions in the wiggler will be of the order  $r_1 \equiv \sqrt{\gamma\epsilon\beta_+} / \gamma = \sqrt{10^{-4} \cdot 10^4} / 4 \cdot 10^5 = 1.6 \cdot 10^{-3} \text{ cm}$ . The  $10\sigma$  criteria gives  $10 \cdot r_1 = 0.016 \text{ cm}$  or  $0.16 \text{ mm}$ , what gives the idea about possible aperture of the wiggler and also an influence of the field inhomogeneities across the aperture.

We will be interesting in the number of the photons emitted by the particle on the  $n$ -th harmonic in the range of relative frequency from  $s = 1$  (corresponding the straight forward direction), to the threshold value  $s = s_*$ . This threshold value defined by the maximal possible angle of incoming radiation, selected by the diaphragm  $\gamma\vartheta = \sqrt{(1 + K^2)(1 - s_*)} / s_*$ . The number of the photons radiated in the range discussed is

$$N_n(K, s_*) = \int_{s_*}^1 \frac{dN_n}{ds} ds = 4\pi\alpha n M \frac{1 + K^2}{K^2} \int_{s_*}^1 F_n(K, s, s_*) ds = 4\pi\alpha n M \frac{1 + K^2}{K^2} \Phi_n(K, s_*, s_*).$$

In approximation  $\kappa = 2K\sqrt{s(1-s)/(1+K^2)} \leq 1$  ( $K \leq 1$  or/and  $\gamma\vartheta \leq 1$ ) for harmonics with the numbers  $n = 1, 2$  one can obtain [11]

$$\Phi_1(K, s_*) = \frac{1}{6}(1 - s_*)(2 - s_* + 2s_*^2) - \frac{K^2}{2(1 + K^2)}(1 - s_*)^2 \left( \frac{4}{15} + \frac{8}{15}s_* - \frac{1}{5}s_*^2 + \frac{2}{5}s_*^3 \right)$$

$$\Phi_2(K, s_*) = \frac{K^2}{10(1 + K^2)}(1 - s_*)^2 \left[ (1 + 2s_* - 2s_*^2 + 4s_*^2) - \frac{20K^2(1 - s_*)}{21(1 + K^2)} \left( \frac{2}{15} + \frac{2}{5}s_* + \frac{4}{5}s_*^2 - s_*^3 + 2s_*^4 \right) \right].$$

The number of the photons on the first and second harmonic as a function of  $K$ ,  $s_*$  is represented on Fig. 6A, Fig. 6C and Fig. 6B.

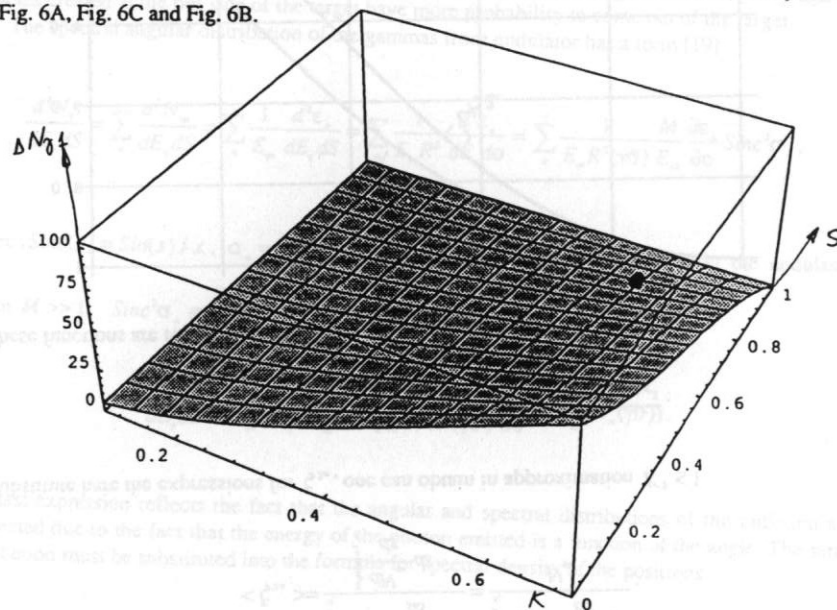


Fig. 6A. The number of the quanta radiated on the first harmonic as a function of  $K$  and  $s = \omega_+ / \omega_{max}$  in all possible energy range.

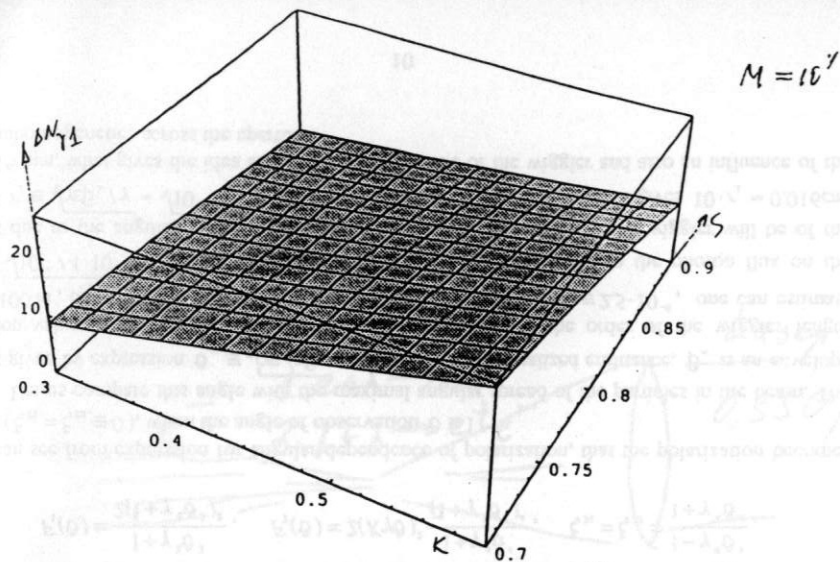


Fig. 6B. The number of the quanta radiated on the first harmonic as a function of  $K$  and  $s = \omega_s / \omega_{max}$  in the interval what may be interested for practical conversion system.

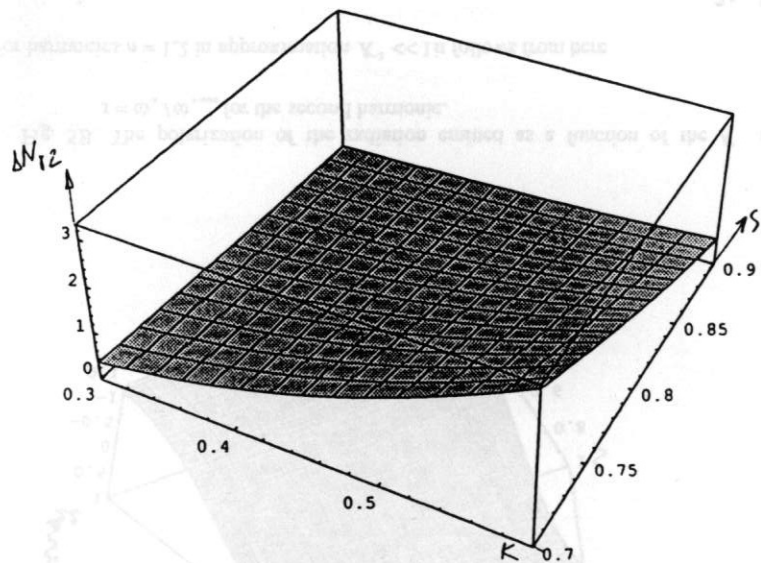


Fig. 6C. The same as above for the second harmonic.

For preparing the gamma flux of maximal possible polarization, the angular separation is necessary. That formally gives the same threshold parameter in description of mean level polarization of the flux.

An averaged value of circular polarization of the photons concentrated in the solid angle between 0 and  $\gamma\theta$ ,  $= \sqrt{(1+K^2)(1-s)}/s$ , can be evaluated as

$$\langle \xi_{2n} \rangle = \frac{\int_0^1 \xi_{2n}(s) \frac{dN_n}{ds} ds}{\int_0^1 \frac{dN_n}{ds} ds} = \frac{\int_0^1 \xi_{2n}(s) \frac{dN_n}{ds} ds}{N_n}$$

Substitute here the expressions for  $\xi_{2n}$ , one can obtain in approximation  $K^2 \leq 1$

$$\langle \xi_{21} \rangle = \frac{3s_1}{2-s_1+2s_1^2}, \quad \langle \xi_{22} \rangle = \frac{5s_1}{1+2s_1-2s_1^2+4s_1^3}$$

These functions are represented on Fig. 7.

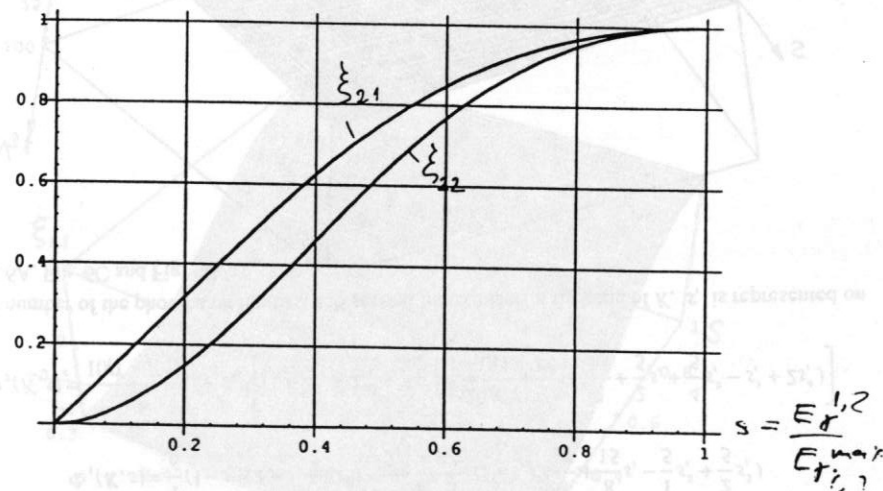


Fig. 7. The averaged polarization of the photon flux as the function of the energy interval of selection.  $s=0$  corresponds to the absence of any selection,  $s=1$  corresponds to the straight forward direction.  $s=0.8$  corresponds to selection in 20% of the energy interval down from the maximal possible energy of the quanta for corresponding harmonics

If selection system collects only in the energy interval 20% of maximal possible energy down from the maximum, i.e.  $s \cong 0.8$ , then  $\langle \xi_{21} \rangle \cong 0.96$ ,  $\langle \xi_{22} \rangle \cong 0.95$ . For  $s \cong 0.7$  (30% interval)  $\langle \xi_{21} \rangle \cong 0.92$ ,  $\langle \xi_{22} \rangle \cong 0.89$ . These figures indicates that the level of polarization is rather high.

The corresponding maximal values of the angles for selection (minimal value is zero for the forward direction) are

$$\vartheta(s=0.7) = \frac{\sqrt{(1+K^2)(1-s)/s}}{\gamma} \cong \frac{0.65\sqrt{1+K^2}}{\gamma} \text{ and } \vartheta(s=0.8) \cong \frac{0.5\sqrt{1+K^2}}{\gamma}$$

If the distance  $L$  between the end of helical wiggler and the target is  $L = 200 \text{ m}$ ,  $\gamma = 4 \cdot 10^3$  (200 GeV),  $1/\gamma \cong 2.5 \cdot 10^{-4}$ ,  $K^2 = 0.25$ ,  $s \cong 0.8$ , then the corresponding radius of the diaphragm at the face of target need to be  $r_0 \cong L \cdot \vartheta \cong 2.8 \cdot 10^{-2} \text{ cm}$ , what gives the diaphragm diameter 0.56 mm.

So, in the *first approximation*, the level of polarization of the positrons created, can be estimated by averaging the function  $f(E_+, E_-)$ , describing the longitudinal polarization of the positron

$$\langle \bar{\zeta}_1 \rangle \cong \langle \bar{\zeta}_2 \rangle \cdot \langle f(E_+, E_-) \rangle \cdot \bar{n}_1$$

For  $E_+, E_- > E_{\text{max}}/2$ , where  $E_{\text{max}} = E_{\text{max}}(s) = s\hbar\omega_{\text{max}} - 2mc^2$ , the function  $f(E_+, E_-)$  can be approximated

$$f(E_+, E_{\text{max}}) \cong 1 - 2 \left( \frac{E_{\text{max}} - E_+}{E_{\text{max}}} \right)^2 = 1 - 2 \left( \frac{s\hbar\omega_{\text{max}} - 2mc^2 - E_+}{s\hbar\omega_{\text{max}} - 2mc^2} \right)^2 = 1 - 2(1-x)^2,$$

where  $x = \frac{E_+}{E_{\text{max}}}$ . By averaging this expression one can obtain

$$\langle f(E_+, E_{\text{max}}) \rangle = \frac{\int_{\Delta} [1 - 2(1-x)^2] dx}{\int_{\Delta} dx} = 1 - \frac{2}{3}(1-\Delta)^2,$$

where  $\Delta = \frac{E_{\text{cap}}}{E_{\text{max}}}$ ,  $E_{\text{cap}}$  is the minimal energy of the positron, captured by the focusing system after the target. For  $E_{\text{cap}} \cong 0.5E_{\text{max}}$  (the positrons in the energy interval 50% down to the maximal possible energy)  $\langle f(E_+, E_{\text{max}}) \rangle = 1 - \frac{2}{3}(1-0.5)^2 = 0.83$ , so

$$|\langle \bar{\zeta}_1 \rangle| \cong \langle \bar{\zeta}_2 \rangle \cdot \langle f(E_+, E_-) \rangle \cong 0.96 \cdot 0.83 = 0.8$$

i.e. rather high level of polarization. In next approximation we need to take into account that there are few of particles with maximum energy according to the  $G(E_+, E_-)$  dependence

$$|\langle \bar{\zeta}_1 \rangle| \cong \frac{\int_{E_{\text{cap}}}^{E_{\text{max}}} \bar{\zeta}_2(E_+) f(E_+, E_-) \frac{d\sigma(E_+, E_-)}{dE_+} dE_+}{\int \frac{d\sigma(E_+, E_-)}{dE_+} dE_+}$$

where  $N_+$  is the number of the energy interval from the maximal possible  $E_{\text{max}} = sE_{\text{max}} - 2mc^2$  to  $E_{\text{cap}}$ . Notice here that the energy distribution must be taken in the moment of pair production without recalculation with the probability  $W$ . The changing of the  $\zeta_1$ , when the particle goes from the point of creation  $\tau$  to the output surface of the target is described by the length of depolarization  $l_{\text{dep}} \cong 3X_0$  [17], so  $\zeta_{\text{out}} = \zeta_1 \cdot \exp(-\frac{\delta - \tau}{3X_0})$ , and the final expression has a form, what includes the spectral properties of the photon flux

$$|\langle \bar{\zeta}_1 \rangle| \cong \frac{1}{8} \frac{\iiint \int_{E_{\text{cap}}}^E \bar{\zeta}_2(E_+) f(E_+, E_-) \frac{d\sigma(E_+, E_-)}{dE_+} \frac{d^2N_+}{dE_+ dS} \exp(-\frac{7}{9}\tau) \exp(-\frac{\delta - \tau}{3X_0}) dE_+ d\tau dE_- dS}{\int \frac{d\sigma(E_+, E_-)}{dE_+} \frac{d^2N_+}{dE_+ dS} \exp(-\frac{7}{9}\tau) dE_+ d\tau dE_- dS}$$

We will see, that the thickness of the target is of the order of  $\delta \leq X_0/2$ , so the factor of radiativ depolarization in the target after creation is less than  $\exp(-\frac{1}{2 \cdot 2 \cdot 3}) \cong 1 - \frac{1}{12} \cong 0.917$ , where additional factor 1/2 reflects the mean path length of the individual positron in the target. Numerical calculations shows that the mean path length even less than 1/2 reflecting the total tendency that the particles created at the out side of the target have more probability to come out of the target.

The spectral angular distribution of the gammas from undulator has a form [19]

$$\frac{d^2N_+}{dE_+ dS} = \sum \frac{d^2N_+}{dE_+ dS} = \sum \frac{1}{E_+} \frac{d^2\epsilon_+}{dE_+ dS} = \sum \frac{1}{E_+ R^2} \frac{d^2\epsilon_+}{dE_+ d\theta} = \sum \frac{1}{E_+ R^2 (\gamma\theta)} \frac{M}{E_+} \frac{\partial \epsilon_+}{\partial \theta} \text{Sinc}^2 \sigma_+$$

where  $\text{Sinc}(x) = \text{Sin}(x)/x$ ,  $\sigma_+ = \pi n M \frac{(\omega - \omega_+)}{\omega_+}$ ,  $M$  is the number of periods in the undulator.

When  $M \gg 1$ ,  $\text{Sinc}^2 \sigma_+ \cong \frac{E_+}{M} \delta(\omega - \omega_+(\gamma\theta))$ , so

$$\frac{d^2N_+}{dE_+ dS} = \frac{1}{E_+} \frac{d^2\epsilon_+}{dE_+ dS} = \frac{1}{\hbar\omega_+(\gamma\theta)} \frac{1}{R^2 (\gamma\theta)} \frac{\partial \epsilon_+}{\partial \theta} \delta(\omega - \omega_+(\gamma\theta))$$

The last expression reflects the fact that the angular and spectral distributions of the radiation are connected due to the fact that the energy of the photon emitted is a function of the angle. The same distribution must be substituted into the formula for spectral density of the positrons

$$\frac{d^2N_+}{dE_+ dS} = \frac{1}{\sigma_{\text{tot}}} \int \frac{d\sigma(E_+, E_-)}{dE_+} \frac{d^2N_+}{dE_+ dS} \cdot \exp(-\frac{7}{9}\tau) W(E_+, E_{\text{max}}, \delta - \tau) d\tau dE_- dE_+ dS$$

Exactly speaking, the formulas represented above are valid is the case when the distance  $L$  from the end of the wiggler to the target is much bigger, than the length of the wiggler itself

$L_u = M\lambda_u \ll L$ . Otherwise we need to average the flux density falling onto fixed point over different angles of coming radiation arising from the different positions of radiated electrons along the undulator. The geometry of averaging is represented on the following Fig. 8.

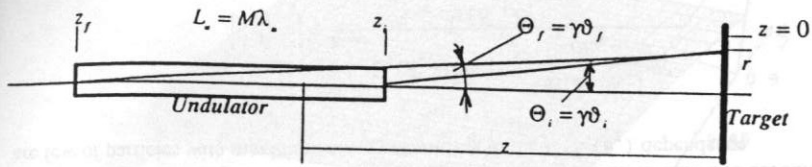


Fig. 8. The geometry of irradiation of the target, when the distance from the end of the undulator is comparable with the length of the undulator itself.  $z = 0$  corresponds to position of the target,  $z_l$  corresponds to beginning of the undulator,  $z_l$  corresponds to its end.

So the spectral density of the energy falling onto the converter's area  $dS$  becomes [11,12]

$$\frac{d^2 N_m}{dE_\gamma dS} \rightarrow \frac{1}{L_u} \int \frac{d^2 N_m}{dE_\gamma dS} dz = \frac{1}{M\lambda_u} \int \frac{1}{R^2(\vartheta)} \frac{\partial N_m}{\partial \omega} \delta(\omega - \omega_*(\vartheta)) dz = \frac{1}{M\lambda_u r} \int \frac{\partial N_m}{\partial \omega} \delta(\vartheta - \vartheta(\omega_*)) \frac{\partial \vartheta}{\partial \omega} d\vartheta$$

where it was used that the angle  $\vartheta$  is connected with the transverse coordinate  $r$  of the point on the target surface (see Fig. 8) by the relation  $\vartheta = -\tan^{-1}(\frac{r}{z}) \cong -\frac{r}{z}$ . In the same approximation it was used, that  $R(\vartheta) \cong z$ ,  $\frac{dz}{z^2} = -\frac{d\vartheta}{r}$ . Substituted also  $\delta(\omega - \omega_*(\vartheta)) = \delta(\vartheta - \vartheta(\omega_*)) \cdot \frac{\partial \vartheta}{\partial \omega}$ . Using

the relations  $\frac{\partial N_m}{\partial \omega} = 4\alpha n M \frac{s^2 \gamma^2 K^2}{(1+K^2)^2} F_s(K, s)$  and expressing the frequency with the parameter  $s$  used above one can finally evaluate the number of photons irradiating the target on  $n$ -th harmonic [11,12]

$$N_m = 2\pi \iint \frac{dN_m}{dS dE_\gamma} dS dE_\gamma = \frac{4\pi\alpha\gamma K^2}{\lambda_u (1+K^2)^{3/2}} \int_0^{z_l} r q_n(K, r_n) dr = \frac{4\pi\alpha\gamma K^2}{\lambda_u (1+K^2)^{3/2}} Q_n(K, r_n)$$

where  $q_n(K, s) = \frac{n}{r} \int \sqrt{\frac{s}{1-s}} F_n(K, s) ds$ ,  $s_i = \frac{1}{1 + \frac{\gamma^2 (r/z_i)^2}{1+K^2}}$ ,  $s_f = \frac{1}{1 + \frac{\gamma^2 (r/z_f)^2}{1+K^2}}$  and  $r_n$  is the radius of the target (the radius of the diaphragm installed before the target). For the first harmonic

$$N_{n1} = \frac{4\pi\alpha\gamma K^2}{\lambda_u (1+K^2)^{3/2}} \left[ \frac{1}{2} \frac{\gamma^2 r_n^2}{\sqrt{1+K^2}} \left( \frac{1}{z_f} - \frac{1}{z_i} \right) - \frac{5\gamma^3 r_n^4}{24(1+K^2)^{3/2}} \left( 1 + \frac{4}{5} \frac{K^2}{1+K^2} \right) \left( \frac{1}{z_f^3} - \frac{1}{z_i^3} \right) \right]$$

For the number of the positrons created in the energy interval  $\Delta E_{\infty} = E_{\infty}^{max} - 2mc^2 - E_{\infty}^{min}$  by the undulator radiation on the  $n$ -th harmonic one can obtain

$$\Delta N_{..}(E_{\infty}^{min}, E_{\infty}^{max}) \cong \frac{\alpha K^2 \delta}{c\gamma \log(183Z^{-1/3})} \Gamma_n$$

where

$$\Gamma_n = \int_0^{z_l} dr \int_{s_i}^{s_f} \frac{F_n ds}{\sqrt{s(1-s)}} \int_{E_{\infty}^{min}}^{E_{\infty}^{max}} G(E_*, E_{\infty}^{max}) \hat{Y}(E_*, E_{\infty}^{min}) dE_*$$

$$\hat{Y} = \frac{1}{\delta} \int_{E_{\infty}^{min}}^{E_{\infty}^{max}} dE_* \int_0^{\delta} I(E_*, E_{\infty}^{min}) d\tau = \frac{1}{\delta} \int_{E_{\infty}^{min}}^{E_{\infty}^{max}} dE_* \int_0^{\delta} \exp(-\frac{\tau}{9}) W(E_*, E_{\infty}^{min}) \delta - \tau d\tau$$

and function  $\hat{Y}$  defines the share of the positrons produced with the energy  $E_*$  that have the out energy in the interval  $\{E_*, E_{\infty}^{min}\}$ . One can evaluate [11]

$$\hat{Y} \left( \frac{E_*}{E_{\infty}^{min}} \right) \cong \frac{\ln 2}{\delta \ln \Delta} (1 - \Delta^{4/n^2})$$

where  $\Delta \cong \frac{E_* - E_{\infty}^{min}}{E_*}$ . For thin target  $I(E_*, E_{\infty}^{min}) \cong \delta(E_* - E_{\infty}^{min})$  and hence  $\hat{Y} = 1$ . Finally

$$\Delta N_{..}(E_{\infty}^{min}, E_{\infty}^{max}) \cong \frac{\alpha K^2 E_{\infty}^{max} \delta Q_n}{c\gamma n \log(183Z^{-1/3})} \int G(\zeta) d\zeta$$

where  $\zeta_{\infty} = \frac{E_{\infty}^{max} - 2mc^2}{s_i E_{\infty}^{max} - 2mc^2}$ . For  $n=1$ ,  $r_n = \kappa z_f = \kappa z_l \frac{\sqrt{1+K^2}}{\gamma}$  the evaluation is the following

$$\Delta N_{n1} \cong 3 \cdot 10^{-3} \kappa^2 M \delta \frac{K^2}{1+K^2} \frac{z_l}{z_i} (1 - \zeta_{\infty})$$

For  $\kappa = 1/2$ ,  $M = 10^4$ ,  $\delta = 0.2$ ,  $K = 1$ ,  $z_f = M\lambda_u = 2z_l$ ,  $\zeta_{\infty} = 0.7$   $\Delta N_{n1} \cong 5$ .

The formulas represented above gives to anyone a possibility to estimate the number of the photons, its average polarization and the number of positrons and its average polarization.

**Codes for calculation** the efficiency of the photons interaction with media. We interrupt here for discussion about existing numerical codes what are able to do this. First of all there are the codes used for modeling the high energy physics phenomena, for example EGS type codes [18 a-b]. The output file of UNIMOD2 (an analog of EGS) is used by the code CONVER [18c] for rather fast calculations with the targets having a different size and form. This output file, obtained on the big computer, having typically 2 MB of memory and describing the individual history of about 6000-10000 incoming photons (depending of the accuracy required), can be preloaded in a Personal Computer. For example, the 486DX-2 66 MHz notebook computer requires about 5 minutes (including the input) to obtain efficiency as a function of the thickness of the target. In [13] described some further modifications, including the codes, which uses the output files from CONVER for the further analysis such as energy distributions, space and angular distribution, distribution of the path lengths, polarization in the target and so on. All these codes also working on

PC. Below the results, obtained with these codes, are described [13]. The main output of these considerations that the efficiency of the particle production could be made around 6% for each initial photon. The mean polarization can reach 70% total.

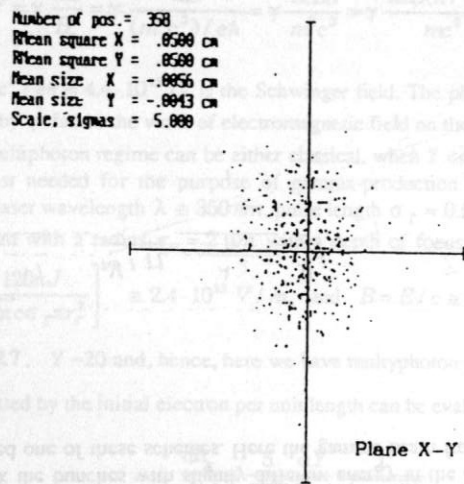


Fig.9 The transverse space distribution of the positrons at the output surface of the target.

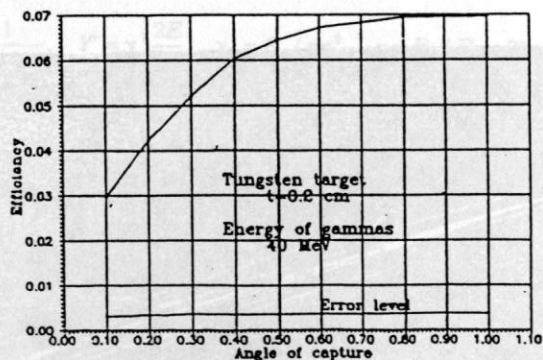


Fig.10. Efficiency of the pair production as a function of the captured angle.

Some special considerations was made to estimate the energy deposition in the material of the target. It was found that this value is around 250 Mev/gram at the end of the target. The thickness of the target was about 0.2 cm. This yield the temperature gain of the order 116 deg for the beam with  $10^{10}$  positrons in the bunch.

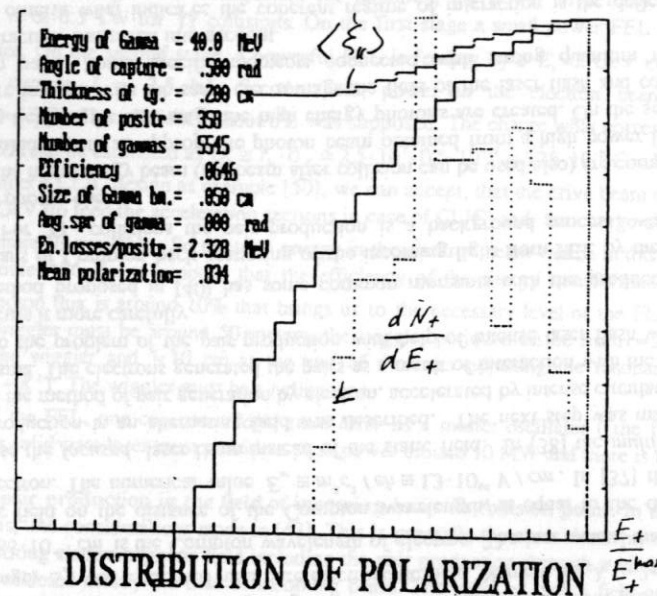


Fig. 11. The energy distribution and polarization. The energy distribution is shown at the moment of positron creation.

The technical proposition for helical field generation was made in [20]. This is a bifilar helix with currents opposed. There are some computer codes for the helical field design [21]. Basically it the same as the codes for calculation of two dimensional fields, but with substitution of coordinate dependence

$$\xi = x + iy \rightarrow \xi e^{-i\omega t} = \xi \cdot \exp(-i2\pi \frac{z}{\lambda_u})$$

what is, basically, the twist with the wiggler period.

The progress in design of short period wigglers with high field one can find in [22-24]. In [24] the results of calculations and testing the models with the period 0.7 and 1 cm are represented. The photography of the tested superconducting undulator is represented on Fig.12. One interesting moment what can be noticed here is that this undulator was supplied with the captured flux. That was made with the help of superconducting transformer. The current in one of 22 turn coil was around 200 A. The impulse undulator (0.7 cm period) has a current around 10 kA with the pulse duration about 50  $\mu$ sec. the voltage was 1.19 kV.

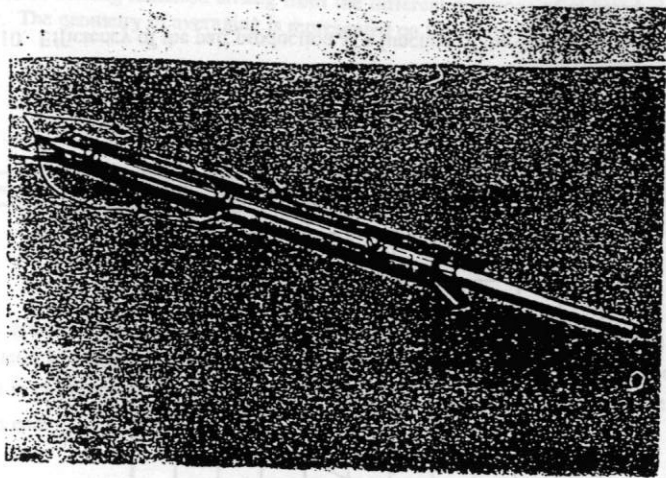


Fig. 12. The 30 cm long superconducting undulator with period 10 mm and the axis field  $\sim 5$  kG.

The wall illumination was considered in [25]. The resistive wall instability if the beam, moving in the vacuum chamber of the wiggler considered in [26]. This looks as weak requirement.

One interesting possibility is connected with further utilization of the gamma beam, passed through a thin converter. The attenuation coefficient  $k = \exp(-7/9\tau)$  for  $\tau = 0.5$  is around 0.68, so in principle the second target can be used as well [13]. The combining schemes is based on the possibility to stack the bunches with slightly different energy in the longitudinal space. On Fig. 13 there is represented one of these schemes. Here the gamma beam from the wiggler is coming from the



Fig. 13. The combining scheme.

left side and illuminates the target T. The focusing lens L collects the particles and adjusts for further optics. An acceleration section  $A_1$  gives the energy  $E_1$  for the secondary beam. This beam of positrons is bent with the help of magnet  $M_1$ . The magnets  $M_1$  and a part of the magnet  $M_2$  with the quadrupoles  $l$  make an achromatic parallel shift of the first beam [27]. The second acceleration section  $A_2$  gives to the beam, collected from the second target, the lower energy  $E_2$ . The magnet  $M_2$  with the part of the magnet  $M_1$  and the lenses, adjusted for parallel shift of the beam with the energy  $E_2$ . The difference in the path lengths of these two lines is an integer of the wavelength and a half of the section  $A_1$ . This section eliminates the energy difference. D is the gamma beam dump.

2.b. A plane wiggler with a sqew dipole field. One interesting class of wigglers considered in [30-32]. This is so called the wigglers with elliptical polarization. This wigglers can be very effective, unfortunately the numerical analyses was not made yet. The basic interest arises from the possibility to have a big undulatory factor in one plane, while in the other plane the undulatory factor is around 1. this can reduce the length of the wiggler.

Micropole wigglers described in [35]. There is no visible applications for its utilization in polarized particle production.

2.c. Collection of the particles with the help of flux concentrator and the lithium lens one can find in [33-34]. The first selection system described [22] used a lithium lens and a diaphragm as energy separator: the particles with the lower energy was overfocused.

### 3. Pair production in the high external electromagnetic field.

#### 3.a. The laser flash mostly.

*Historical review.* The idea of direct pair generation in vacuum comes from [36], where the critical field strength  $E_c$  was estimated in a pure electrostatic field. Namely  $eE_c \lambda_c = 2mc^2$ , where  $\lambda_c = \hbar/mc = 3.86 \cdot 10^{-11}$  cm is the Compton wavelength of electron. The last means, that the work, made by electric field on the distance of the Compton wavelength, is equal to the doubled rest energy of an electron. The numerical value  $E_c \equiv m^2 c^3 / e \hbar \equiv 1.3 \cdot 10^{16}$  V/cm. In [37] the proposal made, how to use the *focused* laser beam instead of the static field. In [38] the *multi-photon*, or *coherent* pair production in an alternating field was described. The next step was made in [39], where discussed the method of pair generation by electron, accelerated by intense circularly polarized laser light in plasma. The electrons generated the pairs as a result of interaction with the nuclei. The final approach to the problem of the pair production with help of intense laser flash was made in [40]. Let us discuss it more carefully.

The method proposed in [40] has some common moments with the production of  $\gamma\gamma$  collisions by means of Compton back scattering of the incoming light from FEL by the relativistic electrons [41]. For  $\gamma\gamma$  collisions the pair production is a background process, what yields a restriction in the photon energy.

Generally, the high energy beam (the beam after collision can be used also) are compressed in a small size and collides with an appropriate photon beam obtained from a high power laser of any type. In a strong field on the first stage the high energy photons are created. On the second stage these photons are interact with the same electromagnetic field of the laser flash and converts into electron-positron pairs. Some specific moments connected with strong quantum regime and multiphoton interaction was taken into account.

The main criteria what indicates the coherent regime of interaction is the deflection angle  $\theta_D = \Delta p / p$  compared with the angle of radiation  $\approx 1/\gamma$ . From equation of motion one can obtain  $\Delta p = 2eE/\omega$ , where the influence of the magnetic field as well as the electric field was taken into account. So  $\theta_D = \Delta p / p \equiv \frac{2eE}{\omega mc\gamma}$ . If  $\frac{2eE}{\omega mc} > 1$  then the deflection angle is much bigger than the divergence of radiation, one can describe it as a multiphoton absorption (synchrotron radiation). In a

case when the angle of deflection is less than  $-1/\gamma$ , or  $\frac{2eE}{\omega mc} = \frac{2eE\hbar}{mc^2} = \pm 1$ , then the interaction becomes significant. The last relation also indicates that in this case the work of the electric field on the distance of the wavelength is negligible. Another important parameter what describes the interaction is

$$Y = \gamma \frac{2E}{B_c} = \gamma \frac{2E}{(m^2 c^3) / e\hbar} = \gamma \frac{2eE\hbar}{m^2 c^3} = \gamma \frac{2eE(\hbar / mc)}{mc^2} = \gamma \frac{2eE\lambda_c}{mc^2},$$

where  $B_c = m^2 c^3 / e\hbar = 4.4 \cdot 10^{13} G$  is the Schwinger field. The physical sense of the  $Y$  parameter is the increased by  $\gamma$  factor the work of electromagnetic field on the Compton wavelength  $\lambda_c$  of an electron. The multiphoton regime can be either classical, when  $Y \ll 1$ , or quantum, when  $Y \gg 1$ . For typical laser burst needed for the purpose of gamma-production [40], energy of the laser flash  $J \cong 15 \text{ Joules}$ , laser wavelength  $\lambda \cong 350 \text{ nm}$ , pulse length  $\sigma_T = 0.5 \text{ ps}$  or  $150 \mu\text{m}$  space duration, the focused beam with a radius  $r_F = 2 \mu\text{m}$  with a depth of focus  $70 \mu\text{m}$  yields the electric field value  $E \cong \left[ \frac{120\pi J}{\sqrt{2\pi c \sigma_T \pi r_F^2}} \right]^{1/2} \cong 2.4 \cdot 10^{13} \text{ V/m}$ , and  $B = E/c \cong 0.8 \cdot 10^9 G$ . So, the parameter  $\gamma\theta_D = \frac{2eE}{\omega mc} = 2.7$ ,  $Y \approx 20$  and, hence, here we have multiphoton quantum regime. The number of the photons emitted by the initial electron per unit length can be evaluated [49]

$$\frac{dn_\gamma}{dz} \cong \frac{5}{2\sqrt{3}} \frac{\alpha Y}{\lambda_c \gamma} \frac{1}{\sqrt{1+Y^{2/3}}}.$$

The photons emitted are interact with the same electromagnetic field. The energy spectrum of the pair production is the following [40,43]

$$\frac{d^2 n_{\pm}}{dx dz} = \frac{1}{\sqrt{3\pi}} \frac{\alpha}{\lambda_c \gamma} \left\{ \left[ \frac{1-x}{x} + \frac{x}{1-x} \right] K_{2/3}(\xi) + \int_{\xi}^{\infty} K_{1/3}(z) dz \right\},$$

where  $\xi = \frac{2}{3Y} \frac{1}{x(1-x)}$ ,  $Y' = \gamma' \frac{2E}{B_c}$ ,  $\gamma' = E_1 / mc^2$ ,  $x = E_+ / E_1$ . The number of the positrons can be evaluated

$$\frac{dn_+}{dz} = \frac{1}{\sqrt{3\pi}} \frac{\alpha}{\lambda_c \gamma'} \int_{x_1}^{x_2} \left\{ \left[ \frac{1-x}{x} + \frac{x}{1-x} \right] K_{2/3}(\xi) + \int_{\xi}^{\infty} K_{1/3}(z) dz \right\} dx,$$

where parameters  $x_1, x_2$  defined by possible gates of capture. The typical values of parameters required for the conversion efficiency, based on calculations, made in [40],  $n_{e^+} / n_{e^-} = 4.5$  (full efficiency). This requires the energy of the laser flash around  $J \cong 15 \text{ Joules}$ , laser wavelength  $\lambda \cong 350 \text{ nm}$ , pulse length  $\sigma_T = 0.5 \text{ ps}$  or  $150 \mu\text{m}$  space duration. These figures gives the power required  $W_{\text{peak}} \cong J / \sigma_T = 30 \cdot 10^{11} \text{ W}$  or  $30 \text{ TW}$ . This is about 100 times more than the power required for  $\gamma\gamma$  collisions. For electron energy  $E_e \cong 250 \text{ GeV}$ , the necessary emittance for focusing electron beam to the transverse dimension  $\gamma\epsilon \cong 10^{-6} \text{ m} \cdot \text{rad}$ . In the energy interval

$\Delta E_e / E_e \cong \pm 2.5\%$  around  $1.6 \text{ GeV}$ . The polarization could be obtained here by using polarized laser light. At the lower boundary of the spectrum the longitudinal polarization could achieve the level of circular polarization of incoming radiation. The other useful possibility in this method, is that for positrons created, the emittance is even less than the emittance of incoming electron beam by a factor 0.03, defining the small angle of created positrons  $\cong 1/\gamma'$ .

Let us estimate the possibility to obtain a laser flash of such a high energy. In [42] there made a consideration for two stage FEL arrangement for obtaining the power in a flash light around  $W_{\text{peak}} \cong 3 \cdot 10^{11} \text{ W}$  or  $0.3 \text{ TW}$  for  $\gamma\gamma$  collisions. On the first stage a small power FEL is using as a master oscillator. On the second stage, a powerful FEL is feeding by a  $E_e = 2 \text{ GeV}$  electron beam with a peak current  $I_e = 2.5 \text{ kA}$ . So the peak power in the electron beam is around  $W_{\text{beam}} \cong I_e \cdot E_e = 5 \text{ TW}$ . The efficiency about 6% was supposed. The charge what corresponds to the current of  $2.5 \text{ kA}$  can be estimated as  $Q_e \cong I_e \cdot \sigma_T = 2.5 \cdot 10^3 \cdot 0.5 \cdot 10^{-12} \cong 1.25 \cdot 10^{-9} \text{ C} = 1.25 \text{ nC}$ .

If we consider a CLIC design as example [50], we can accept, that the drive beam of the energy around  $E_e = 3 \text{ GeV}$  (to feed the acceleration sections in case of CLIC) and the charge about  $Q_e = 40 \text{ nC}$  (and even more) is available. So the total energy in the electron beam will be in this case around  $E_e Q_e = 120 \text{ Joules}$ . So if one suppose that the efficiency of the energy transformation from the beam to the photon flux is around 10% that brings us to the necessary level of the FEL flash. The length of the wiggler must be around 50 meters, the wiggler period must be from  $\approx 20 \text{ cm}$  at the beginning of the wiggler and  $\approx 10 \text{ cm}$  at the end of the laser adjusting the resonant frequency  $\lambda_e \cong 2\lambda\gamma^2 / (1+K^2)$ . The wiggler must be a helical one.

Instead the FEL, one can use a *solid state laser* as a master oscillator (the first stage of amplifier). This solid state laser must provide a peak power around  $10 \text{ MW}$  and there is no limitation to get it.

**3.b. The pair production in the field of incoming beam in collision point.** In the same line of investigations, the considerations made in [43]. This is generally the exact description of the pair production in strong electromagnetic field including the pair production through a virtual photons. The authors considered mostly the field of incoming beam. The value of such a field can reach the order of MG. So the  $Y$  parameter can reach the level of tens. However the polarization is not available due to absence of controlled polarized statements in this reaction.

**4. Natural polarization in a damping ring.** In [44,45] a self polarization due to synchrotron radiation is predicted. The time dependence of polarization could be described by the formula

$$P(t) = P^- (1 - \exp(-\frac{t}{\tau_p})),$$

where the asymptotic level of polarization  $P^- = \frac{8}{5\sqrt{3}} \cong 0.9238$  and the characteristic time of polarization is

$$\tau_p = \frac{8m|\rho|^3}{5\sqrt{3}r_0\hbar\gamma^3} \cong \frac{8 \cdot mc^3 |\rho|^3 e^2}{5\sqrt{3} \cdot e^2 r_0 \hbar c^2 \gamma^3} = \frac{8|\rho|^3 \alpha}{5\sqrt{3}r_0^2 \gamma^3 c},$$

where  $\rho$  is a bending radius in the magnetic field. This time can be compared with the time of radiation damping

$$\tau_{\text{rad}} = \frac{3}{2} \frac{\rho^2}{r_0 \gamma^3 c}.$$

So the ratio of these times is

$$\frac{\tau_p}{\tau_{\text{rad}}} = \frac{16|\rho|\alpha}{15\sqrt{3}r_0\gamma^2}.$$

Even simple radiation damping of the emittance is a problem due to high repetition rate required. One can see that the huge factor  $|\rho|/r_0$  cannot be neutralized. So, self polarization is not useful for the purposes of preparing the beam.

5. Cleaning the beam in the damping ring by blowing out the positrons with unnecessary polarization with the polarized laser beam.

The proposal was made [46] to illuminate the beam in a damping ring by a laser light with appropriate polarization. Due to dependence of cross section of the polarization one can hope to kick out the positrons (or electrons) with unnecessary polarization.

So only half of positrons are rest. Not taking into account the time of the process, what depends of the intensity of the light, one can estimate that this is an extremely extensive way.

6. Radioactive decay.

The radioactive decay [47] is not able to provide the necessary amount of positrons, having appropriate brightness. Remember, the average power of the beam is a few megawatts.

7. Discussion, Conclusion.

In conclusion we can say that for future linear colliders the method of polarized particle production with the help of circular radiation from the undulator or wiggler looks attractive. The typical length of helical wiggler for production one polarized particle per one initial is about 100 meters. The degree of polarization could achieve 70%. There is no apparent limitation to applying this method.

The method of positron production using conversion of the high intensity laser beam comes to difficulty to find a source of such powerful flash. The FEL scheme looks as the only possibility to do this.

Very attractive may be utilization of the wigglers with elliptical polarization. This requires more detailed calculations.

$$E \approx 200 \text{ GeV}$$

$$L \approx 100 \text{ M}$$

$$\lambda_u \approx 1 \text{ cm}$$

$$\frac{N_{e^+}}{N_{e^-}} \approx 1 \quad (1.5 \text{ if combine})$$

$$\sigma_E \approx 5 \cdot 10^{-2} \text{ m rad}$$

$$\xi_H \approx 0.7$$



- [23] A.A. Anashin et al., "Superconducting helical undulator for measurements of polarization of interacting beams in VEPP-2M storage ring", Preprint INP 84-11, Novosibirsk, 1984.
- [24] T.A. Vsevolozskaya, A.A. Mikhailichenko, E.A. Perevedentsev, G.I. Silvestrov, A.D. Cherniakin, "Helical Undulator for conversion system of the VLEPP project", XIII International Conference on High Energy accelerators, August 7-11, 1986, Novosibirsk.
- [25] A.A. Mikhailichenko, Dissertation, INP, Novosibirsk, 1986.
- [26] A.A. Mikhailichenko, V.V. Parkhomchuk, "Transverse resistive instability of a single bunch in a linear collider", Preprint INP 91-55, Novosibirsk, 1991.
- [27] K. Steffen, "High Energy Beam Optics", Interscience publishes, 1965.
- [30] E.G. Bessonov, E.B. Gaskevich, "About the Spontaneous and Induced Radiation of the particles on higher harmonics in the undulator with elliptically polarized magnetic field", Brief reports on Physics FIAN, 1985, No. 8, p.17-21.
- [31] S. Yamamoto, H. Kitamura, "Generation of quasi-Circularly Polarized Undulator Radiation with higher Harmonics", Japanese Journal of Applied Physics, vol. 26, No. 10, Part 2, October, 1987, pp. L1613-L1615.
- [32] H. Onuki, N. Saito, T. Saito, "Undulator generating any kind of elliptically polarized radiation", Appl.Phys. Lett. 52(3), p. 173, 18 January 1988.
- [33] A. Kulikov, LC -93, SLAC, Stanford, 1993.
- [34] G.I. Silvestrov, "Problems of production high intensity beams of secondary particles", XIII International Conference on High Energy Accelerators, August 7-11, 1986, Novosibirsk.
- [35] P. L. Cshonka, NIM A, Vol 345, No 1, 1994.
- [36] J.Shwinger, Phys Rev. 82, 664 (1951); 93, 615 (1954).
- [37] F.V. Bunkin, I.I. Tugov, "Possibility of creating Electron-Positron Pairs in a vacuum by focusing of the laser radiation, Soviet Physics-Doklady, Vol.14, No. 7, 1970. Translated from Doklady Akademii Nauk SSSR, Vol. 187, No.3, pp541-5444, July 1969. Submitted December 24, 1968.
- [38] E. Brezin, C. Itzykson, "Pair production in Vacuum by an alternating field", Phys. Rev. D, Vol.2, No.7, 1070.
- [39] J.W. Shearer, J. Garrison, J. Wong and J.E. Swain, "Pair production by relativistic electrons from an intense laser focus", Presented at the Third Workshop on "Laser Interaction and Related Plasma Phenomena", held at Rensselaer Polytechnic Institute, Troy, New York, August 13-17, 1973.
- [40] P. Chen, R.B.Palmer, "Coherent Pair Creation as a Positron Source for Linear Colliders", In AIP Conference proceedings N 279, "Advanced Accelerator Concepts", Port Jefferson, NY, 1992, p.888.
- [41] A.M. Kondratenko, E.V. Pakhtusova, E.L. Saldin, Dokl. Akad. Nauk 264(1982) 849, Preprint INP 81-130, Novosibirsk (1981), in Russian.
- [42] E.L. Saldin, V.P. Sarantsev, E.A. Schneidmiller, M.V. Yurkov, "FEL based Photon Collider of TeV Energy Range", Preprint of JINP E9-94-70, Dubna, 1994 ( Submitted to "Particle Accelerators").
- [43] V.N. Baier, V.M. Katkov, V.M. Strakhovenko, "On the Electroproduction of  $e^+, e^-$  pairs in the external Field", Journal of Nuclear Physics, vol. 53, N 4, 1991.
- [44] I.M.Ternov, Yu. M. Loskutov, L.I. Korovina, Sov. Phys. JETP. 14 (1962)1921.
- [45] A.A. Sokolov, I.M.Ternov, Sov. Physics Doklady, 8,(1964)1203.
- [46] V.N. Baier, a private communication. More exact reference is unknown.
- [47] "Methods of Experimental Physics", L. Morton, editor, Academic Press 1963.
- [48] B. Rossi, "High Energy Particles", N/Y, 1982.
- [49] J.Spencer, IEEE Conf. Proc. No. 91CH3038-7,5,3270 (1991).
- [50] The CLIC Study group, "The CERN Linear Collider", Proc. of the 1993 Particle Accelerator Conference, Washington, May 1993, also CERN/SL 93-20 (DI) and CLIC Note 195.

## 8. References.

- [1] See the talks represented on LC -93, SLAC, Stanford, 1993.
- [2] A.A. Likhoded, M.V. Shevlyagin, O.P. Yushchenko, "Mass bounds on the extra neutral vector bosons at future  $e^+, e^-$  colliders with polarized beams, International Journal of Modern Physics A, Vol. 8, No. 28 (1993), pp. 5063-5077.
- [3] K. Flottmann, "Required parameters for S-band and TESLA", this Workshop.
- [4] H. Braun, "Required parameters for X-band and CLIC", this Workshop.
- [5] B. Montague, "Polarized beams in high energy storage rings", Physics reports, Vol. 113, No 1, November 1984.
- [6] V.B. Berestetzky, E.M. Lifshitz, L.P. Pitaevsky, "Quantum electrodynamics, Moscow Nauka, 1989, vol.4.
- [7] A.A. Mikhailichenko, "Obtaining and operation with the polarization on VLEPP", III Int. Workshop on High energy Physics, Protvino, 5-8 Sept. 1989, IHEP publishing, 1990, pp.444-446. pin handling
- [8] a). VLEPP Linear Collider Physical design report, Novosibirsk, INP, 1979.  
b). B.W. Montague, "Polarized Beams in the CERN Linear Collider?", CLIC Note 35, March 1985.
- [9] E.A. Kushnirenko, A.A. Likhoded, M.V. Shevlygin, "Depolarization effects for collisions of the polarized  $e^+, e^-$  beams", preprint IHEP 93-131, Protvino, 1993, (Submitted to Sov. Journ. Nucl. Phys.).
- [10] V.E. Balakin, A.A. Mikhailichenko, "Conversion system for obtaining highly polarized electrons and positrons", Preprint INP 79-85, Novosibirsk 1979.  
V.E. Balakin, A.A. Mikhailichenko, "VLEPP: the conversion system", Proc. of the 12 Int. Conference on high energy Accelerators, Batavia, 1983, p. 127.
- [11] E.G. Bessonov, A.A. Mikhailichenko, "Some aspects of Undulator radiation forming for conversion system of the linear collider", Preprint INP 92-43, Novosibirsk, 1992.
- [12] E.G. Bessonov, "Some aspects of the theory and technology of the conversion systems of linear Colliders", International Conference on High Energy Accelerators, Hamburg, 1992, p.138.
- [13] A.D. Bukin, A.A. Mikhailichenko, "Optimized target strategy for polarized electrons and positrons production for linear Collider, Budker INP 92-76, Novosibirsk, 1992.
- [14] K. Flottmann, J. Rossbach, "A High Intensity Positron source for Linear Collider, DESY M-91-11, 1991.
- [15] K. Flottmann, PhD Thesis, DESY, Hamburg, 1993.
- [16] a) W. Heitler, "The Quantum theory of radiation", Oxford University Press, 1954.  
b) A.I. Akhiezer, V.B. Berestetzki, "Quantum electrodynamics", Moscow, Nauka, 1981.
- [17] V.N. Baier, V.N. Katkov, V.S. Fadin, "Radiation of the relativistic electrons", Moscow, Atomizdat, 1973.
- [18] a). EGS  
b) A.D. Bukin, N.A. Grozina, M.S. Dubrovin et al., "UNIMOD2 -Universal Simulating program for  $e^+, e^-$  experiments", Preprint INP 79-149, Novosibirsk, 1979.  
c) A.D. Bukin, "The choice of optimal Positron Converter for low energy beam", Preprint INP 90-100, Novosibirsk, 1990.
- [19] E.G. Bessonov, "Undulators, Undulator Radiation, FELs, M.: Nauka, 1993.-192 p.-(Proc. P.N. Lebedev Phys. Inst.; Vol.214). See also the bibliography in this fundamental monography.
- [20] R.C. Wingerson, "Corkscrew" -a device for changing the magnetic moment of charged particles in a magnetic field, Phys. Rev. Lett., 1961, Vol. 6, No. 9, pp. 446-449.
- [21] A.N. Dubrovin, E.A. Simonov, "MERMAID- MESH-oriented Routine for MAGnet Interactive Design", User's guide, Novosibirsk, INP, 1992.
- [22] A.D. Cherniakin et al. "The development of the conversion system for VLEPP project", ibid., p.131.

Talk:

Alexander Novokhatski

Budker Institute of Nuclear Physics

WG 2

## Electron-Positron Preinjector Complex at Novosibirsk

A.V. Novokhatski, A.V. Alexandrov, M.S. Avilov, O.Yu. Bazhenov, Yu.M. Boimelshtain, N.S. Dikansky, I.V. Kazarezov, N.Kh. Kot, A.A. Kulakov, N.A. Kuznetsov, P.V. Logatchov, P.V. Martyishkin, Yu.I. Semenov, A.N. Sharapa, A.V. Shemyakin, S.V. Shiyankov, B.A. Skarbo, A.N. Skrinsky, S.B. Vasserman

Budker Institute of Nuclear Physics, Novosibirsk, 630090, Russia

### Abstract

A complex of electron-positron factories is under construction at Budker Institute of Nuclear Physics (BINP) at Novosibirsk. This paper presents status of preinjector complex, which dedicated for initial production of electron and positron bunches and their acceleration upto energy of 510 MeV.

### INTRODUCTION

Preinjector complex, damping ring and future linear collider VLEPP type linac comprise injector complex of electron-positron factories (Fig.1), which have to provide effective operation of those machines and existing storage rings. Main parameters of preinjector are presented in Table 1. Preinjector output

Table 1. Main preinjector parameters.

Output energy	510 MeV
Number of electrons per bunch	$10^{11}$
Number of positrons per bunch	$10^9$
Repetition rate	50 Hz
Energy spread:	
electron bunch	$\pm 1\%$
positron bunch	$\pm 3\%$
RF frequency	2856 MHz
Klystron pulse power	$\sim 63$ MW
Number of klystrons	4 + 1
Total power consumption	$\approx 1$ MW

energy 510 MeV is an operation energy of  $\Phi$ -factory. A number of  $(5 \div 10) \cdot 10^{10}$  of electrons and positrons per second required for simultaneous operation of  $\Phi$ -factory, VEPP-3, VEPP-4M and VEPP-5 at designed luminosities.

The chosen preinjector scheme had to meet not only scientific requests, but also hard constraints on cost of the project. The decision to place injector

complex and  $\Phi$ -factory inside existing building imposed hard limitations on the area, occupied by preinjector. To achieve required reliability of the machine, basically well proven scientific and technical solutions have been chosen.

### PREINJECTOR SCHEME AND COMPONENTS

Main components of the preinjector are shown in Fig.1. Preinjector consists of thermionic electron gun, subharmonic buncher, 300 MeV electron linac, isochronous 180° turn, conversion system, RF photogun, 510 MeV positron linac and debuncher-monochromator. First 300 MeV linac is used to create intensive electron bunch for positron production. Positrons after conversion system or electron bunch from polarized photogun are accelerated up to 510 MeV in positron linac.

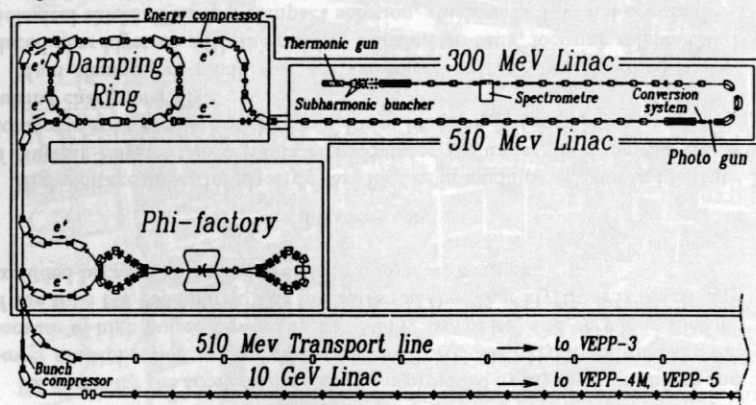


Figure 1. Injector complex and  $\Phi$ -factory

Linacs consist of the four accelerating units. Each unit comprise SLAC S-band klystron 5045, BINP designed and produced klystron modulator, power multiplication system and travelling wave accelerating sections (4 sections, each with 18 MeV/m accelerating gradient, or 3 sections, one with 25 MeV/m and two with 18 MeV/m).

### Thermionic Gun and Bunch Compression System

The thermionic 200 kV triode gun with control grid (triggered pulse of 500 V amplitude) delivered 2 ns pulses with pulsed current 10 A. The emittance of the beam is less than  $10^{-2}\pi \cdot \text{cm} \cdot \text{rad}$  and the transverse size at the crossover after adjusting lenses is 0.5 cm.

Subharmonic buncher, following electron gun, comprise two quarter-wavelength

cavities with drift gaps and compress the bunch in longitudinal direction by factor of more than ten. Cavities operate at the 16th subharmonic of the basic frequency and each is feeded with tube amplifier of 20 kW pulsed power. Transverse focusing of the beam is provided by longitudinal magnetic field, produced by current coils, surrounding cavities. To reduce size of the coils the diameter of the cavities is maximally reduced (up to acceptable reduction of the shunt impedance due to strong capacity load). To keep transverse size of the beam, an amplitude of the magnetic field increases in correspondance with the longitudinal compression of the bunch.

After the second drift gap is placed short section with exponentially growing RF field of the main frequency, where bunch is compressed by another factor of ten.

This bunching system provides short (18 ps) intensive bunches at low initial gun current. Short bunch length is required to provide small energy spread ( $\pm 1\%$ ) during further acceleration.

### 300 MeV Electron Linac and 180° isochronous turn

300 MeV electron linac consist of 5 accelerating sections. Travelling wave accelerating sections of both linacs are of 3 m long and have constant impedance structure operating at  $(2\pi/3)$  mode. To provide the reliable capture of bunches of low energy, first section of 300 MeV linac (and of 510 MeV linac) have a higher accelerating rate of 25 MeV/m and solenoid for transverse focusing of the beam. Regular accelerating sections have 18 MeV/m accelerating gradient and two quadrupole lenses placed on each.

300 MeV electron bunch pass 180° isochronous turn. Bending system consists of three 60° bending magnets and four quadruple lenses. This system provides transport of the bunch with energy spread  $\pm 3\%$  without significant increasing of the bunch length.

### Conversion Target

After 180° turn triplet focus the bunch on the conversion target. Beam spot size on the surface of Tungsten target is about 1 mm. Adiabatic magnetic field was chosen as matching device. This field is produced by the flux concentrator. To obtain realistic numbers for conversion ratio magnetic field of the first accelerating section solenoid, and RF accelerating field have to be taken into account. As the simulations calculations shows, for the 300 MeV electron bunch overall conversion ratio may be higher than 3%. At the 50 Hz repetition rate that's enough to provide required numbers of positron per second.

## Photogun

Typically (approximately 98% of total time) preinjector provides positrons bunches for further cooling and merging in damping ring. Electron bunch produced at once by a photogun. The photogun is placed between focusing triplet and conversion system. To obtain electron beam target have to be removed. Readjustment of the focusing system does not required.

## 510 MeV Positron Linac and debuncher-monochromator

As mentioned above 510 MeV linac almost all the time accelerates positron bunches. It comprise 9 accelerating sections and as 300 MeV linac have first one with 25 MeV/m accelerating gradient within solenoid and regular sections with gradient 18 MeV/m and quadupole focusing system.

Debuncher-monochromator is dedicated for decreasing of initial energy spread of the positrons before injection into the damping ring.

## RF System of Linacs

### Klystron

RF power for the accelerating sections is provided by klystron amplifiers and power multiplication system. As amplifiers SLAC 5045 klystrons were chosen, because of high pulsed power (up to 67 MW per pulse) and very long lifetime of the tube (40 000 hours). The utilisation of the other klystrons is practically excluded because of limited area for preinjector complex.

### Modulator

High-voltage pulses for klystrons are formed in modulators. Now in Institute of Nuclear Physics two variants of modulator are under development: traditional one with oscillatory charge of Pulse Forming Network (PFN) and with pulsing charge of PFN.

Main elements of modulator are assembled withing two shielded boxes, placed near klystron with the pulsing transformer tank, focusing solenoid and biological shield. This is a compact solution, shielded hall do not required. A klystron gallery is separated from the linacs by radiation shield. Besides, the conversion system has the local shield.

## Power Multiplication System and RF Distribution

SLED type power multiplication system allows to obtain required gradients of the accelerating fields, using only four 5045 klystrons. Each klystron with SLED feeds three or four accelerating sections.

First sections of 300 MeV and 510 MeV linacs with accelerating gradient of 25 MeV/m receive half of the microwave power from two corresponding klystrons, second half of this power is divided by two for feeding of two regular sections. The power of two other klystrons is divided equally between four regular sections. RF power divided by means of 3db couplers. Necessary phase shift between accelerating sections, connected to one klystron, is provided on high power level by the phase shifters, made from mechanically squeezable waveguide. The phasing of klystrons and their power level regulation is carried out at the low power level by the adjustable phase shifters and attenuators on the input of each klystron.

## CURRENT STATE OF THE PREINJECTOR

Simulation on the beam dynamic and the field electrodynamic, conversion system currently carried out, the design of the main preinjector elements is completed.

Control and data acquisition system for the preinjector complex is under developing. It is based on utilising intellectual CAMAC controllers on INMOS transputers. Net of transputer controllers will be supervised by higher level computer under UNIX operating system, providing operator interface, etc..

Construction and furnish of the radiation protected tunnel for linacs, klystron gallery and control room of preinjector complex is completed. The constructions of radio control room is almost completed. The creation of general infrastructure and engineering support of the preinjector are in progress.

The prototypes of the accelerating section, focusing system, subharmonic buncher and the power multiplication cavities are made. The "cold test" of separate microwaves elements are carried out.

The installation and setup of separate elements of the preinjector has begun: 100 keV electron gun prototype, subharmonic generators and focusing coils for subharmonic buncher (see Fig.2).

Tests of the 100 keV electron gun, focusing coils for subharmonic buncher, power multiplications resonant cavities are in progress.

The first 5045 klystron was successfully delivered from SLAC and assembled under supervision and comprehensive assistance of Dr. Ron Koontz during his visit to Novosibirsk. At the same time the water load was mounted and all devices for measurements of RF power were installed. The klystron assembly (see Fig.3) is now prepared for connection to modulator and further testing. The first modulator for 5045 klystron is assembled and is now under commissioning. The high voltage power supply, pulse form network and charging choke were tested. The first "hot" test of all modulator are planed at the end of this year. The general view on the klystron gallery is shown in Fig.4.

Talk:

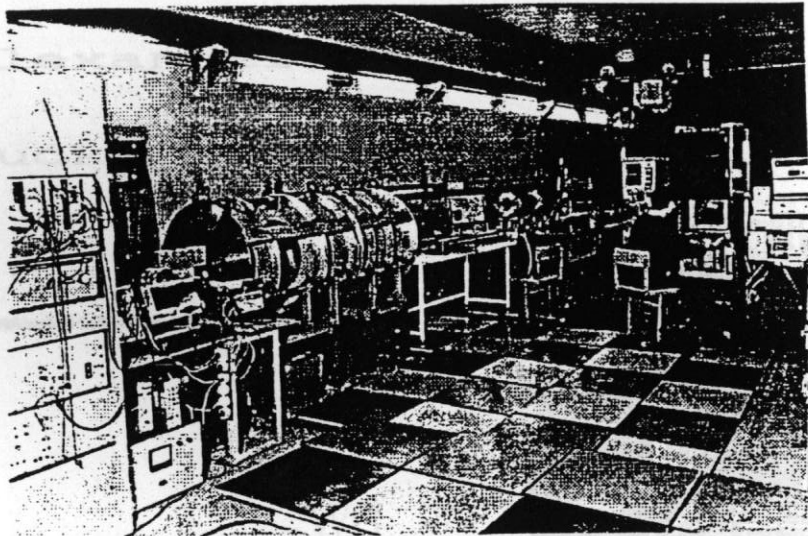


Figure 2. Linacs Tunnel

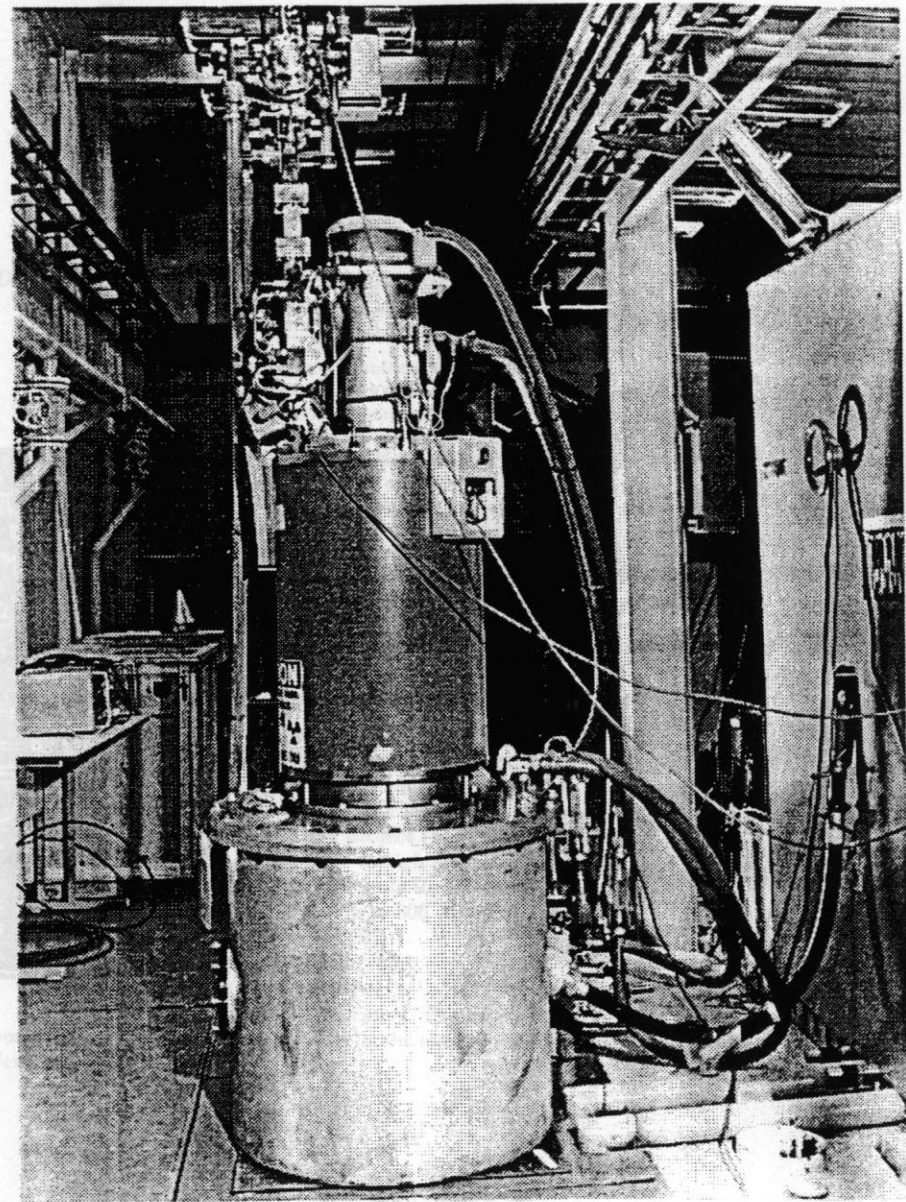


Figure 3. Klystron 5045

-459-

### Protogun

Typically (approximately 80% of total time) protogun provides positrons for further cooling and merging in damping ring. Electron bunch produced at once by a discharge. The protogun is placed between focusing triplet and extraction system. To obtain electron beam target have to be removed. Adjustment of the focusing system does not required.

### 310 MeV Positron Linac and dephaser-monochromator

Accelerator above 10 MeV uses almost all the linac. It consists of 3 accelerating sections and an 300 MeV section. It consists of 3 accelerating sections and an 300 MeV section. It consists of 3 accelerating sections and an 300 MeV section. It consists of 3 accelerating sections and an 300 MeV section.

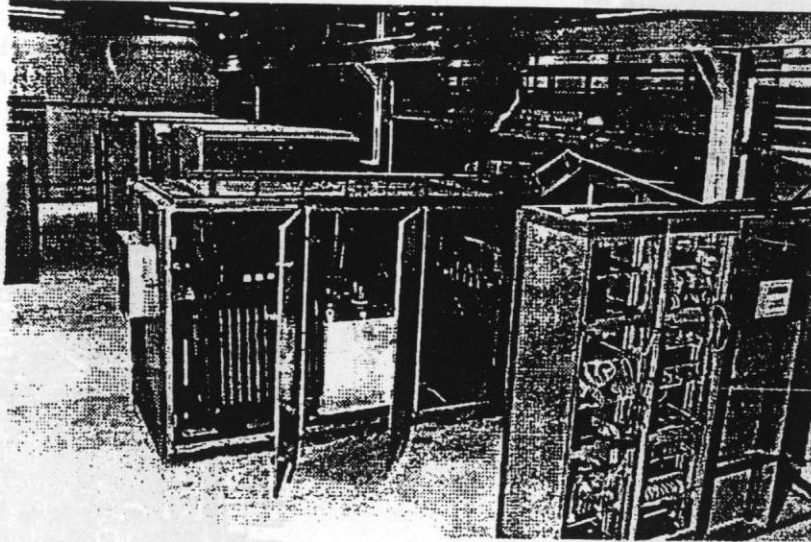


Figure 4. Klystron Gallery

First sections of 300 MeV... accelerating gradient of 25 MeV/m... klystrons... sections... shift... high... wave... out

-497-

Power Multiplication System and RF Distribution  
4:1 type power multiplication system allows to obtain required gradients for accelerating units using only four 300 kV klystrons. Each klystron with 1000 kV peak-to-peak accelerating voltage.

power... unit... visit... dem... for... The... ch... of the

Talk:

Alexander Novokhatski

Budker Inst. of Nucl. Phys.

### Short bunches from GaAs Photocathode

A.V.Novokhatski, A.V.Aleksandrov, M.S.Avilov, P.V.Logatchev.  
Institute of Nuclear Physics, 630090 Novosibirsk, Russia.

R.Calabrese and V.Guidi.

Dipartimento di Fisica dell'Universita and INFN, I-44100 Ferrara, Italy.

G. Lamanna, G.Guillo and B.Yang.

Laboratori Nazionali di Legnaro, I-35020 Legnaro, Italy.

L.Tecchio.

Dipartimento di Fisica Sperimentale dell'Universita and INFN, Torino, Italy.

#### Abstract

A gun with a laser-triggered photocathode is very attractive as an electron source for linear accelerators since it can produce low-emittance and intensive beam. Additional opportunity gives GaAs photocathode, that can generate a polarized electron beam. The optimum way of realization of the gun is a crystal inside RF cavity. However it could be possible if the time response of GaAs photocathode is short enough and comparable with RF period. An experimental facility has been fabricated to measure the length of electron bunch extracted from GaAs photocathode illuminated by short laser pulse. The method of bunch length measurement using circular scanning in RF cavity was developed. Also the same cavity provides bunch length measurement using wake fields, excited in the cavity by travelling bunch. In this report the description of experimental set-up and obtained results are presented.

#### Introduction

Future electron-positron colliders require a very high luminosity and, therefore, a sufficiently large number of injected particles. A laser-driven RF gun appears to be the most convenient electron source which is able to supply a very high intensity. It is planned to use a laser-driven RF gun at the injector complex for Novosibirsk Phi-factory project (1). This electron source can produce short and intensive bunches due to high fields available in RF gun. GaAs photocathode satisfies all the requirements for the electron beam:

- A very high current densities - up to  $800 \text{ A/cm}^2$ .
- High quantum efficiency - up to 20%.
- High degree of polarization (upto 100%).
- Reasonable life time - up to few weeks.

Several problems still need to be solved. The direct and returned electron bombardment, high vacuum and the main question is time response dependence upon current.

WG 2

-494-

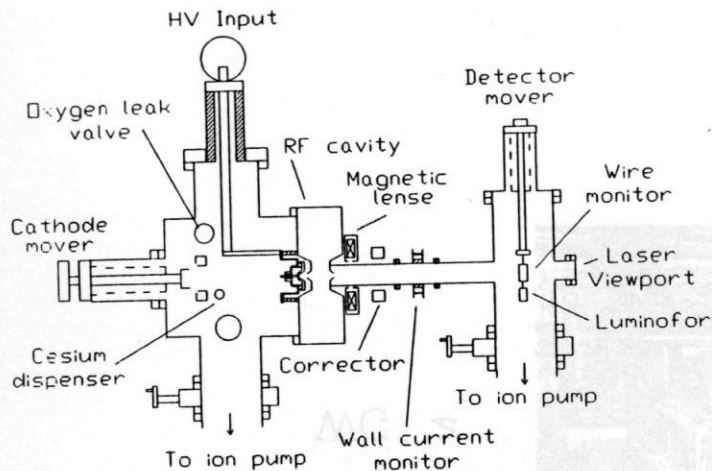


Figure 1. Experimental setup.

### Experimental setup

For direct production of short bunches experimental setup was constructed. The GaAs photocathode (p-doped by Zn,  $10^{19} \text{cm}^{-3}$ ) is prepared in NEA condition by depositing Cs and  $\text{O}_2$  at its surface with a standard procedure in preparation chamber (2). When activation has been accomplished, the cathode is fastened to the DC gun by manipulator (see Fig.1). This procedure allows to avoid the problems of sparking due to Cs covering of the high voltage surfaces.

The cathode is negatively biased with a voltage ranging within 0-80 kV. The diameter of the laser spot on the cathode is around 2 mm, and gun perveance is  $1.5 \cdot 10^{-3} \frac{\text{A}}{\text{kV}^{3/2}}$ .

Photoemission is excited by a CW laser of 6 - 75 mW  $\text{Ar}^+$  for activation, and a pulsed (532 nm) Mode-Locked Nd:YLF laser. A pulsed laser provides the minimum laser beam length of 40 ps with a 10 Hz repetition rate. An autocorrelator is used for a control of laser pulse duration (FWHM) with 10 ps accuracy.

The main idea of the method for bunch length measurement is in circular scanning of electron beam travelling in rotating magnetic field, excited in RF cavity. The electrons passing through the cavity along its axis experience transverse deflection, which direction depends on the longitudinal position of electron in the bunch. As a result longitudinal position of electrons is transformed to angular position in the plain orthogonal to the axis.

$TM_{110}$  modes are used and circular polarization is provided by exciting of

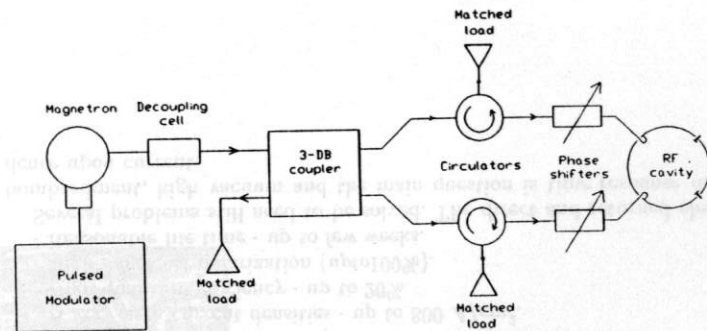


Figure 2. RF scheme of installation.

two orthogonal modes shifted on  $\frac{\pi}{2}$  in phase. RF scheme is presented in Fig. 2. The beam with duration  $\Delta\tau$  sweeps in the plain orthogonal to the axis an arc of circumference with sizes:

$$R = \frac{eH_0\lambda \cdot L}{\pi\gamma mc^2}$$

$$\Delta\theta = w \cdot \Delta\tau$$

where  $\lambda$  is RF wavelength,  $w$  - frequency and  $H_0$  is an ampl. of magnetic field. We can determine the beam duration  $\Delta\tau$  by measuring the angular size  $\Delta\theta$ . Let us consider the main sources of error in this procedure.

1. The final size of the beam. If the beam has final transverse size  $d$  on the detector then its duration can be determined with uncertainty  $\delta\tau$ :

$$\frac{\delta\tau}{T} = \frac{d}{2\pi R} \quad (1)$$

where  $T$  is period of RF

2. The energy distribution in the beam produces the uncertainty :

$$\frac{\delta\tau}{T} = \frac{1}{4} \cdot \frac{1}{2 + \frac{3U}{W_0} + \left(\frac{U}{W_0}\right)^2} \cdot \frac{\delta U}{U} \quad (2)$$

where  $U$  is accelerating voltage,  $W_0 = 511 \text{ keV}$ .

3. If orthogonal modes have difference in amplitude  $\delta H$  and phase shift differs from  $\frac{\pi}{2}$  to  $\delta\phi$ , then polarization of resulting magnetic field is elliptical. In this case the error in determination of bunch duration depends on the bunch duration and azimuth of bunch center of mass but doesn't exceed :



$$\frac{\delta\tau}{T} \leq \sqrt{\left(\frac{\delta H}{H_0}\right)^2 + (\delta\phi)^2} \quad (3)$$

Cavity was optimized to get maximum deflection of the beam with 50KV energy for given input RF power. The resonant frequency is 2.46GHz, measured unloaded quality factor is 17000. The cavity has two orthogonal loops for RF power input and two piston tuners for adjustment of resonant frequency of each mode in the range  $\pm 0.5$  MHz. Pulsed magnetron is used as the source of RF power. Its power and frequency can be controlled in some range by amplitude of anode pulse from modulator. The maximum power is 2.0 KW. The stable operation of magnetron is provided by ferrite circulator which decouples magnetron from resonant load. The adjustment of cavity is performed by using continuous electron beam. When polarization is circular, electron beam draws a full circle on the detector surface and makes a uniform charge distribution on the channels of  $2\pi$ -detector. The direct observation of deflected continuous electron beam is also possible on luminescent screen which can be moved under beam instead of  $2\pi$ -detector.

The  $2\pi$ -detector is a set of 30 tantalum sectors perpendicular to the beam axis with a hole for laser beam in the center. Each sector acts as a Faraday cup to collect the electrons of the bunch. The maximum resolution of this instrument is  $400/30=13.3$  ps, and normal electronic noise of ADC is  $10^6$  electrons per each channel. For a total charge measurement we use a Faraday cup and a wall-current monitor.

### Experimental results

Typical distribution of the charge in the bunch is shown in Fig.3. The shape of laser beam measured by autocorrelator is also given at this picture. Shapes of laser beam and electron bunch are comparable if number of electrons is in the range of several units of  $10^8 e^-$ , however with charge increasing bunch length increases. Observed lengthening could not be explained by the space charge flight time effect.

Another possibility for bunch length measurement is in investigation of wake fields, induced by electron beam in "empty" cavity. Signals of output power from crystal detector are presented in Fig4. If the bunch length is in the range when two first modes are excited mainly, then output power can be described by sum of two exponents with different decay times. In this approach it is possible to calculate the amplitudes of excited modes and to determine the bunch length. Measured bunch length in assumption of Gaussian shape is shown in Fig.3.

### Conclusion

According to data obtained in this experiment a thick GaAs photocathode has small enough time response. Upper limit for the lengthening of the electron

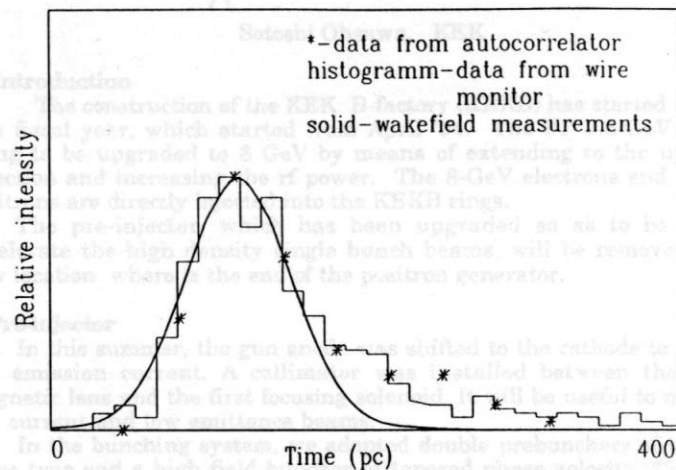


Figure 3. Laser pulse and charge density distribution.

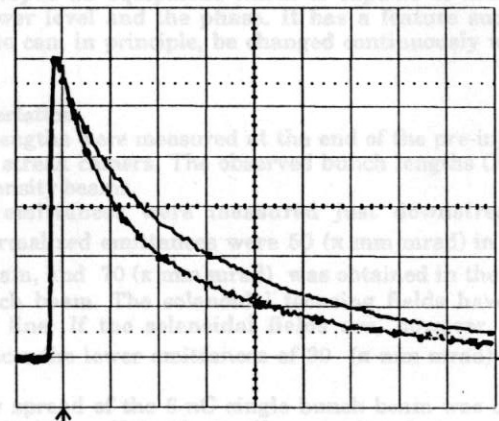


Figure 4. Signals induced in "empty" cavity by electron bunches with different lengths.

bunch due to GaAs time response is less than 30 ps for electron beam with  $2.0 \cdot 10^8 e^-$  particles at energy of 60 kV. Measured bunch length increasing with extracted charge increasing could not be explained by the space charge flight time effect. For getting more detailed information it is necessary to continue this experiment with a laser of shorter beam length.

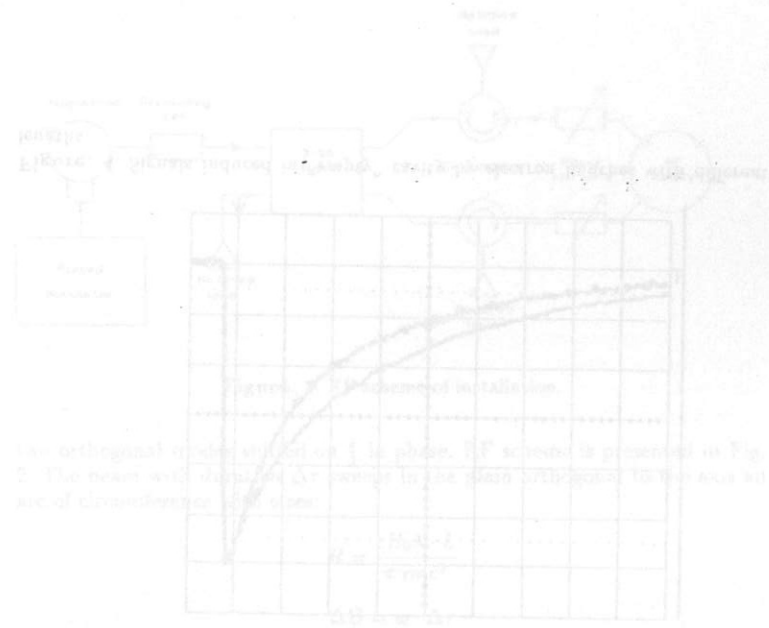
### REFERENCES

1. A.V.Novokhatski, A.V.Aleksandrov, A.A.Kulakov, P.V.Logatchov, L.Tecchio. A laser-driven gun for electron-positron factories. NIM A 340(1994) p.237-240, North-Holland.
2. D.T.Pierce, R.J.Celotta, G.-C.Wang, W.N.Unertl, A.Galejs, C.E.Kuyatt and S.R.Mielczarek; Rev. Sci. Instrum. 51 (1980) 478.

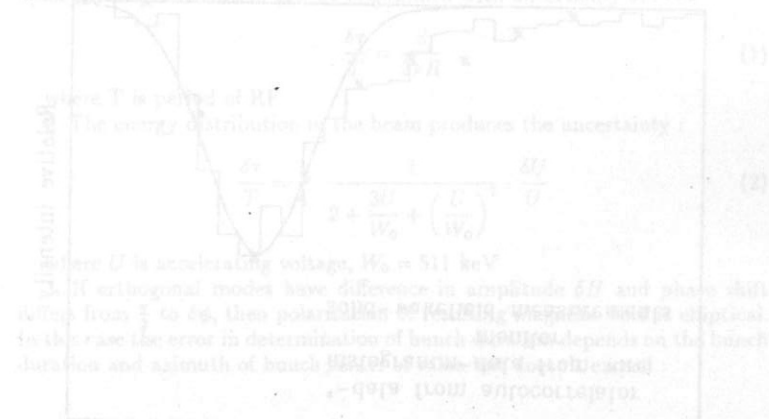
-494-

### Experimental setup

The experimental setup is shown in Fig. 1. The electron beam is produced by a GaAs photocathode gun. The beam is accelerated by a 60 kV DC gun. The beam is then deflected by a magnetic field and passes through a series of apertures. The beam is then detected by a detector. The detector is connected to a computer which records the beam position and size. The computer also controls the magnetic field and the apertures. The beam size is measured by a laser interferometer. The laser interferometer is connected to a photodetector which is also connected to the computer. The computer calculates the beam size and position from the data recorded by the photodetector. The beam size is measured at different distances from the gun. The beam size is found to increase with distance. This is due to the space charge effect. The space charge effect is the repulsion between the particles in the beam. This repulsion causes the beam to expand as it travels. The space charge effect is more pronounced for larger beams and for longer distances. The space charge effect is also more pronounced for lower energies. The space charge effect is a major limitation on the performance of electron guns. It is necessary to find ways to reduce the space charge effect in order to improve the performance of electron guns. One way to reduce the space charge effect is to use a laser-driven gun. A laser-driven gun produces a shorter bunch length than a GaAs photocathode gun. This shorter bunch length reduces the space charge effect. Another way to reduce the space charge effect is to use a higher energy gun. A higher energy gun produces a smaller beam size. This smaller beam size also reduces the space charge effect. A third way to reduce the space charge effect is to use a longer distance. A longer distance allows the beam to expand more before it is detected. This expansion also reduces the space charge effect. The space charge effect is a complex phenomenon and it is still being studied. It is hoped that the results of this experiment will help to improve our understanding of the space charge effect and to find ways to reduce its effects in electron guns.



Let us consider the main sources of error in this procedure. The final size of the beam at the gun has final transverse size  $d$  on the detector, then its location can be determined with uncertainty  $\delta r \approx 100$ .



where  $U$  is accelerating voltage,  $W_0 = 511$  keV. If orthogonal modes have difference in amplitude  $\delta U$  and phase  $\delta \theta$  with  $\delta \theta$  from  $\pi/2$  to  $3\pi/2$ , then polarization of the beam is elliptical. In this case the error in determination of the bunch length depends on the bunch distance and alignment of bunch.

Talk:

Anatoly Sharapa

Inst. of Nucl. Physics

WG 1

### THERMIONIC GUN FOR BINP INJECTOR.

B.I.Grishanov, A.R.Frolov, A.N.Sharapa, A.V.Shemyakin

A thermionic gun with a constant high voltage and a grid-controlled current will be used to produce electrons for the BINP injector.

Main parameters of the thermionic gun.

Energy of electrons, keV	200
Peak beam current, A	10
Pulse duration FWHM, ns	2
Repetition frequency, Hz	50
Emittance, cm <sup>2</sup> rad	< 0.01 pi
Energy spread, keV	< 2
Synchronization precision, ns	< 0.1

The high voltage power supply is the 20 kHz Cockcroft-Walton generator used in BINP ion industrial accelerators. An isolating SF6 gas under a pressure of 1.7 atmosphere is used. The maximum average current of HVPS is 0.1 mA. A constructive capacity is large enough to provide an appropriate energy spread during a pulse.

A cathode-grid block from an industrial tube is used. The BaO cathode has a diameter of 12 mm and needs less than 15 W of heating power. It is necessary to apply approximately 100 V of the grid-cathode voltage to extract 10 A.

The gun electrodes are optimized to minimize an electric field on surfaces.

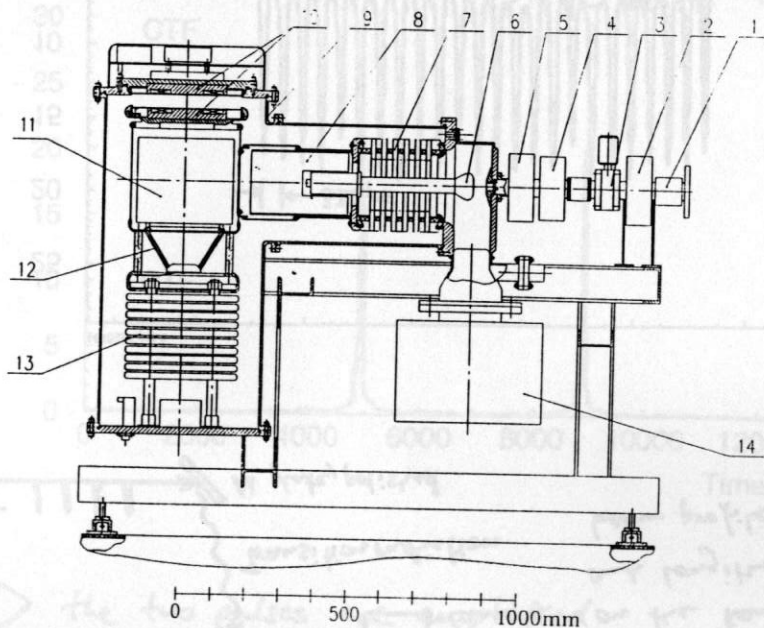


Fig.1. Thermionic gun scheme.  
1- correction coils, 2- second solenoidal lens, 3- vacuum valve, 4- resistive monitor of the beam current, 5- first solenoidal lens, 6- cathode, 7- multigaps insulator, 8- beam current driver, 9- SF6 tank, 10- power transmission transformer, 11- power supplies for the beam current driver, 12- resistors, 13- high voltage power supply, 14- ion pump.

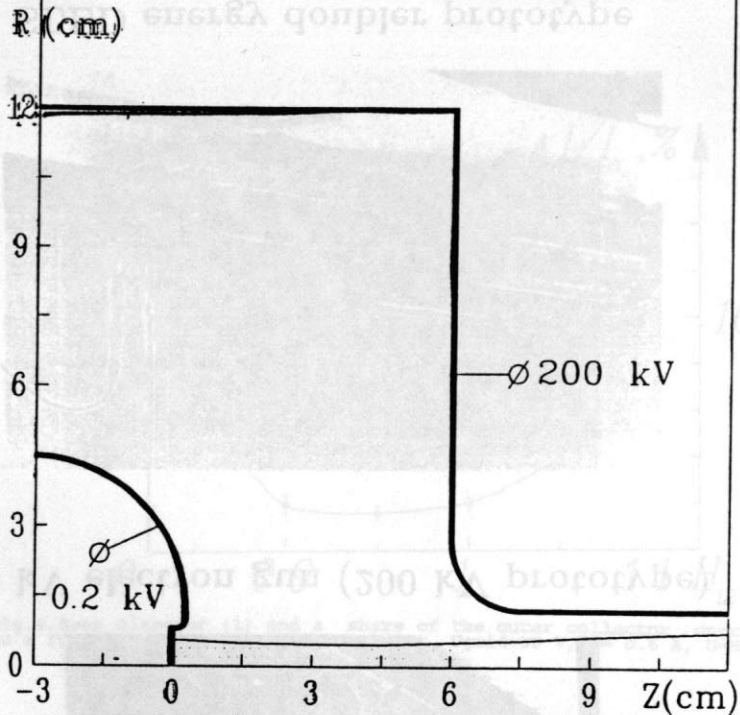
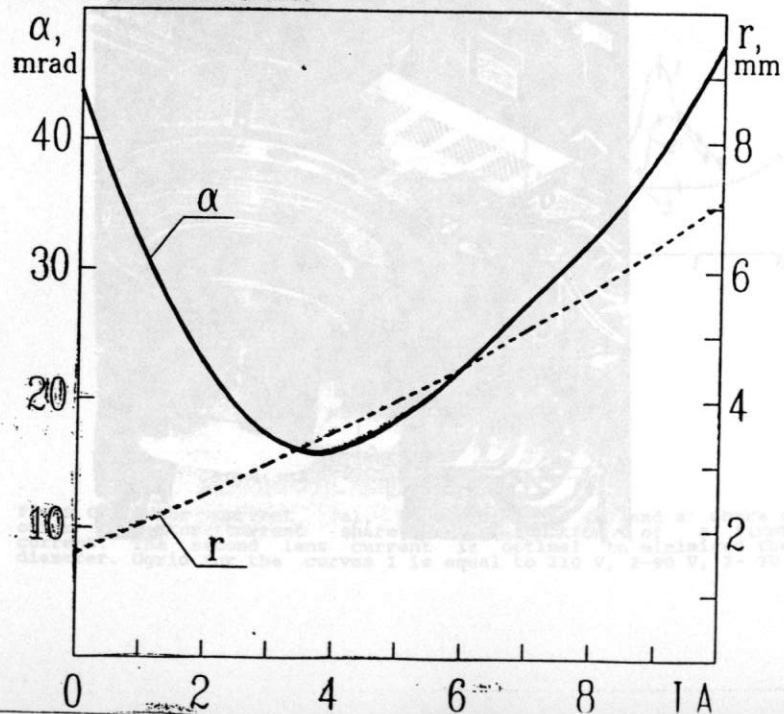


Fig. 2. The gun electrode geometry and the boundary beam trajectory calculated for 10 A beam current.



TEST 100 KV GUN.

In order to test gun elements a 100 kV gun was produced. It has the same cathode-grid block and an air isolation.

Attained parameters of the 100 kV gun.

Energy of electrons, keV	70-100 (depends on air conditions)
Peak beam current, A	3
Pulse duration FWHM, ns	2
Repetition frequency, kHz	up to 5
Emittance, cm*rad	<0.01 pi

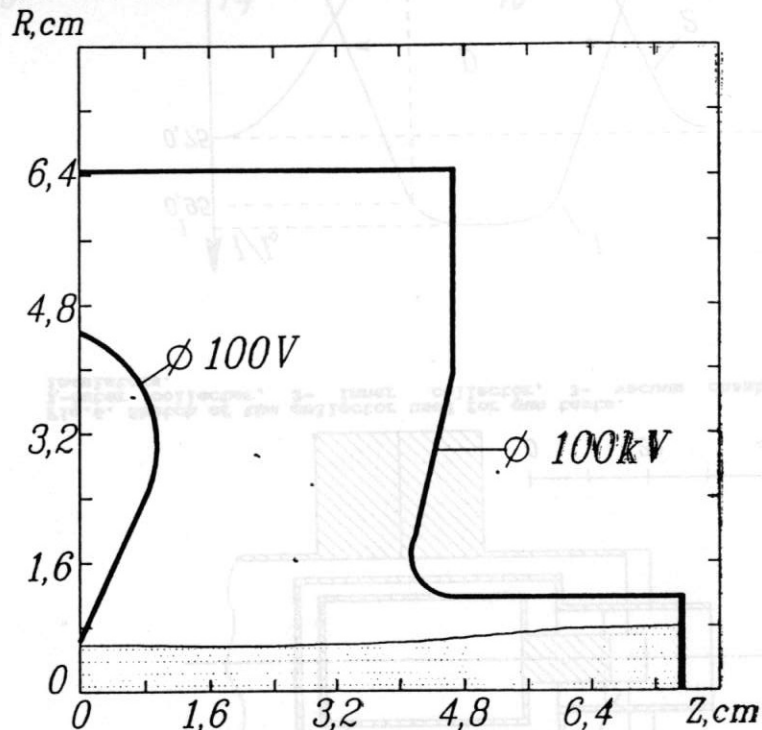
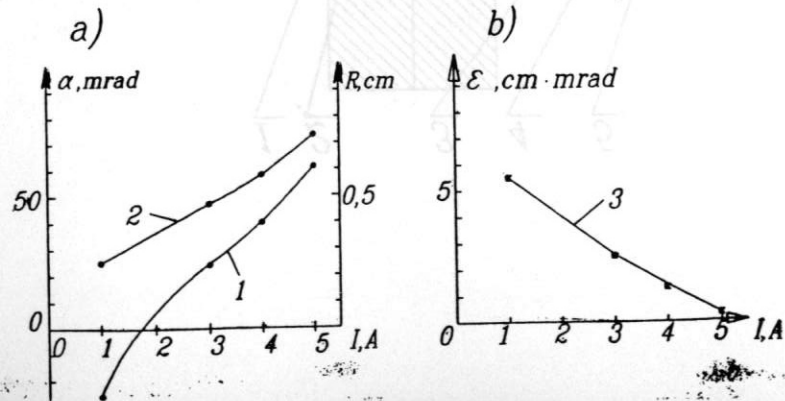
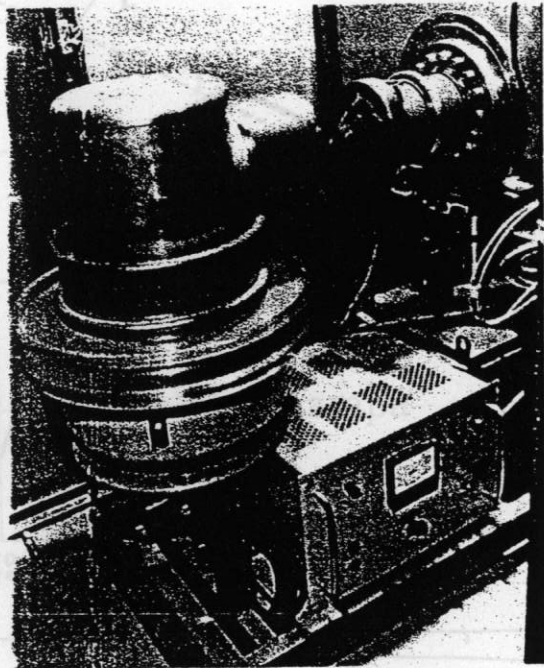
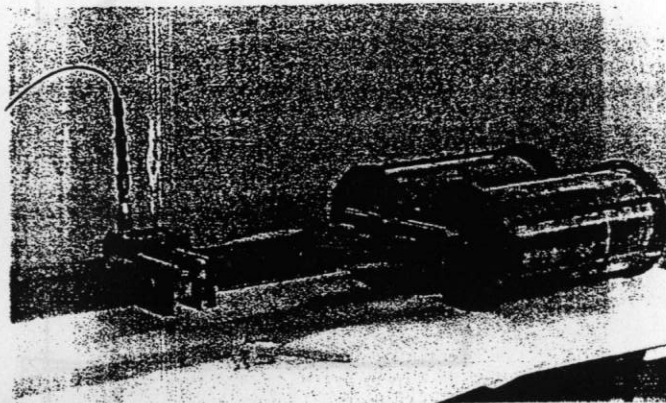


Fig. 4. The 100 kV gun electrode geometry and a boundary trajectory calculated for 5 A beam current.





100 kV electron gun (200 kV prototype)



SLED energy doubler prototype

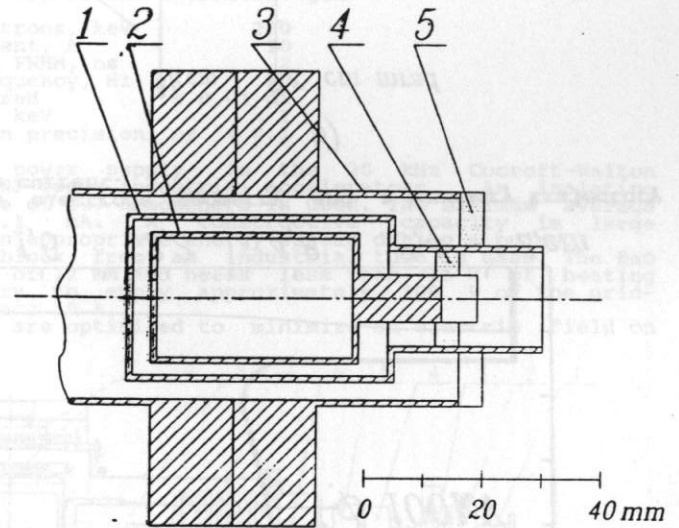


Fig.6. Sketch of the collector used for gun tests. 1-outer collector, 2- inner collector, 3- vacuum chamber, 4,5- insulators.

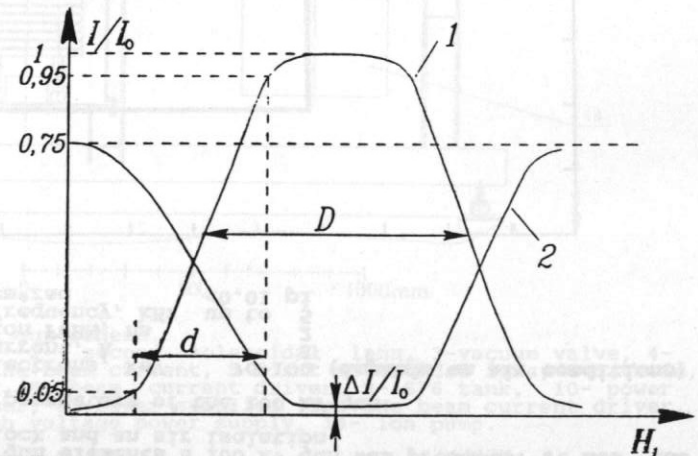


Fig.7. Illustration of a beam dimension measurement method. Curves 1 and 2 are currents of inner and outer collectors, respectively, as a function of a correction coil current. "D" corresponds to the diameter of a hole in the outer collector, "d" corresponds to the beam diameter. A difference in maximums of the currents is due to a secondary electron emission from a outer collector surface with a coefficient 0.25.

Beam emittance

$U_{grid}, V$     $\epsilon, \pi \text{ cm} \cdot \text{mrad}$     $\Delta I/I, \%$

$U_{grid}, V$	$\epsilon, \pi \text{ cm} \cdot \text{mrad}$	$\Delta I/I, \%$
30	1	0.7
90	6	3.4
120	14	10

Requirements:  $V_{102}$  conversion of protons into  $\beta^+$   
capture position with acceptable  
for damping rings

Passible targets

Reaction	Q	decay constant	lifetime
$p + N \rightarrow N + \gamma \rightarrow N + e^+ + \nu$	2.7	0.0001	0.2
$p + Mg^{24} \rightarrow Mg^{24} + \gamma \rightarrow Mg^{24} + e^+ + \nu$	3.2	2.2	9.6
$p + Si^{28} \rightarrow Si^{28} + \gamma \rightarrow Si^{28} + e^+ + \nu$	4.0	9.9	5.1
$p + S^{32} \rightarrow S^{32} + \gamma \rightarrow S^{32} + e^+ + \nu$	4.5	2.5	8.6
$p + Ca^{40} \rightarrow Ca^{40} + \gamma \rightarrow Ca^{40} + e^+ + \nu$	5.6	0.75	6.5

~5% mass difference between stable  
& unstable isotopes - separation should be easy

we calculate 87% of  $e^+$  will be trapped  
on  $\beta^+$  decay

Need to be able to separate from  
difference energy of  $e^+$  for  $\beta^+$

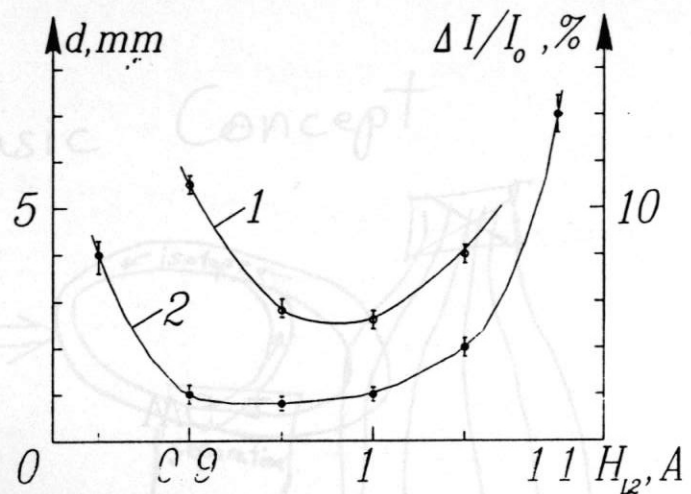


Fig.8. Beam diameter (1) and a share of the outer collector current (2) as a function of a second lens current.  $U_{grid}=30 V, I=0.6 A, U=50 kV$ .

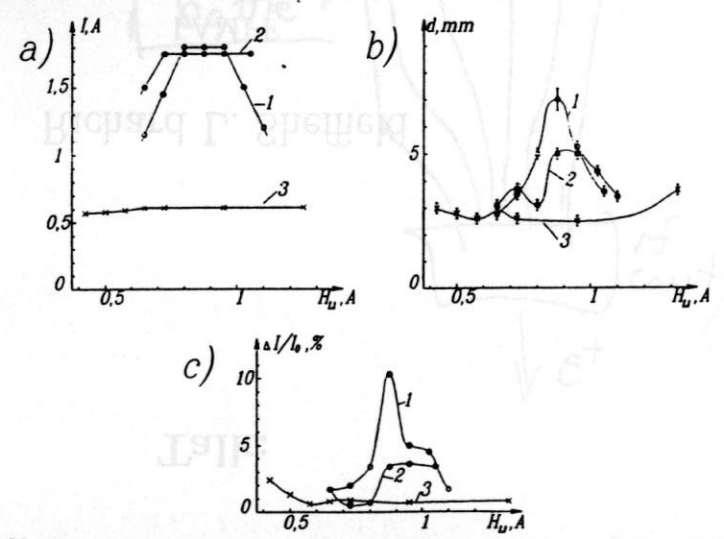


Fig.9. Collector current (a), beam diameter (b) and a share of the outer collector current as a function of a first lens current. The second lens current is optimal to minimized the beam diameter.  $U_{grid}$  for the curves 1 is equal to 210 V, 2-90 V, 3- 30 V.

-553-